

Supporting Information

***P*-Protected Diphosphadibenzo[a,e]pentalenes and Their Mono- and Dicationic *P*-Bridged Ladder-Stilbenes**

Patrick Federmann,^a Hannah K. Wagner,^a Patrick W. Antoni,^a Jean-Marc Mörsdorf,^b José Luis Pérez Lustres,^b
Hubert Wadeohl,^a Marcus Motzkus,^{*b} and Joachim Ballmann^{*a}

^a Anorganisch-Chemisches Institut, Ruprecht-Karls-Universität Heidelberg, Im Neuenheimer Feld 276, 69120 Heidelberg, Germany.

^b Physikalisch-Chemisches Institut, Ruprecht-Karls-Universität Heidelberg, Im Neuenheimer Feld 229, 69120 Heidelberg, Germany.

Table of Contents

Experimental Procedures	S2
Selected NMR Spectra	S4
Selected EPR Spectra and Spin Density Plots	S14
Photophysical Measurements.....	S15
Details on DFT Calculations	S17
X-Ray Crystal Structure Determinations	S31
References	S34

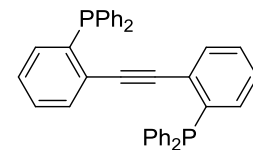
Experimental Procedures

General Remarks

All experiments were conducted under an atmosphere of dry and oxygen-free argon by using standard Schlenk techniques or in a glovebox (MBraun). Argon 5.0 was used and further dried by passing over a column of phosphorus pentoxide. Glassware was heated to 130°C overnight and evacuated while still hot. Dichloromethane, diethylether, hexane, pentane, THF and toluene were purified by a MBraun Solvent Purification System. Deuterated solvents were dried over sodium (benzene-d₆, THF-d₈, toluene-d₈) or over calcium hydride (CD₂Cl₂) and distilled prior to use. Chlorodiisopropyl- and chlorodiphenylphosphine were purified by simple distillation and stored in Teflon-valve ampules. All other chemicals were purchased from commercial suppliers and used as received. 2,2'-Dibromotolane was prepared according to literature.¹ One and two dimensional ¹H, ¹³C and ³¹P NMR spectra were recorded on a Bruker Avance DRX 300, a Bruker Avance II 400 MHz or on a Bruker Avance 600 III spectrometer. Unless noted otherwise, all X-nuclei spectra were recorded with ¹H broadband or composite pulse decoupling. Residual (undeuterated) solvent served as reference for ¹H and ¹³C NMR spectra. Chemical shifts δ are given in parts per million (ppm), coupling constants J in Hertz (Hz). Signal multiplicities are stated by common abbreviations (e.g. s – singlett, d – doublet, dd – doublet of doublets). Mass spectra were recorded at the Department of Organic Chemistry at Heidelberg University on a JEOL JMS-700 magnetic sector by liquid injection FD ionization (LIFDI) technique. Cyclic Voltammetry measurements were carried out on a standard commercial electrochemical analyser in a three electrode single-component cell under argon atmosphere (Pt disc working electrode, platinum wire counter electrode, SCE reference electrode, internally referenced to ferrocene with [NBu₄][PF₆] as supporting electrolyte). Elemental analyses were carried out at the Department of Inorganic Chemistry at Heidelberg University on an Elementar vario MICRO Cube. ESR spectra were recorded on a MagneTech MiniScope MS400 spectrometer or on a Bruker ESP 300 spectrometer. Melting point ranges were determined using a Büchi SMP-20 melting point apparatus.

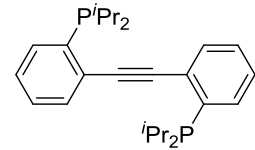
Synthesis of 2,2'-bis(diphenylphosphanyl)tolane (**7a**)

A solution of 1.0 eq 2,2'-dibromotolane (3.36 g, 10.0 mmol) in diethyl ether (125 ml) was cooled to -20°C. A solution (2.5 M in hexane) of 2.0 eq *n*-butyllithium solution (8.00 ml, 20.0 mmol) was added over 10 min. The reaction mixture was stirred for 15 min at -20°C and then for 15 min at 0°C. The resulting pale yellow solution was cooled to -40°C and 2.1 eq chlorodiphenylphosphine (4.63 g, 21.0 mmol) was added dropwise. The reaction mixture was stirred at -20°C for 4h and allowed to warm to room temperature. The solvent was removed *in vacuo*, and the solid residue was suspended in toluene (70 ml) and filtered over silica. The eluent was evaporated and the residue washed with pentane (3 x 10 ml). After drying *in vacuo*, **7a** (4.11 g, 75%) was obtained as colorless powder (mp. 155-165°C with ongoing conversion to **4a**). ¹H{³¹P} NMR (600 MHz, CD₂Cl₂, 22°C): δ (in ppm) = 7.39-7.34 (m, 12H), 7.32-7.30 (m, 8H), 7.24-7.22 (m, 2H), 7.19-7.17 (m, 2H), 7.12-7.11 (m, 2H), 6.79-6.78 (m, 2H). ¹³C{¹H, ³¹P} NMR (CD₂Cl₂, 151 MHz, 22°C): δ (in ppm) = 140.7 (C_q, 2C), 136.9 (C_q, 4C), 134.5 (CH, 8C), 132.8 (CH, 2C), 132.7 (CH, 2C), 129.2 (CH, 4C), 128.9 (CH, 8C), 128.8 (CH, 2C), 128.6 (CH, 2C), 127.9 (C_q, 2C), 95.4 (C_q, 2C). ³¹P NMR (CD₂Cl₂, 242 MHz, 22°C): δ (in ppm) = -9.3 (s). ³¹P{¹H} NMR (161 MHz, CDCl₃, 22°C): δ (in ppm) = -9.3 (s). Anal. Calcd. for C₃₈H₂₈P₂ (546.17 g/mol): C 83.50, H 5.16. Found: C 83.50, H 5.31. The analytical data are in accordance with literature values (**7a** has been prepared previously by Kowalik *et al.* starting from unsubstituted tolane, *n*-BuLi/KO*t*Bu and ClPPPh₂).²



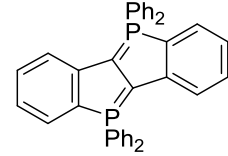
Synthesis of 2,2'-bis(diisopropylphosphanyl)tolane (7b)

Following the procedure for **7a**, 1.0 eq 2,2'dibromotoluene (10.0 mmol, 3.36 g) was reacted with 2.0 eq *n*-butyllithium (20.0 mmol, 1.28 g, 2.5M in hexane) and 2.1 eq chlorodiisopropylphosphine (21.0 mmol, 3.20 g). Workup after 40 h afforded **7b** (3.04 g, 7.41 mmol, 74%) as crystalline off-white solid (mp. 70–80°C with ongoing conversion to **4b**). ¹H NMR (CD_2Cl_2 , 600 MHz, 22°C): δ (in ppm) = 7.67–7.63 (m, 2H), 7.49–7.45 (m, 2H), 7.36–7.31 (m, 4H), 2.27 (septd, $J_{\text{H-H}} = 7.0$ Hz, $J_{\text{H-P}} = 1.7$ Hz, 4H), 1.16 (dd, $J_{\text{H-H}} = 7.0$ Hz, $J_{\text{H-P}} = 14.5$ Hz, 12H), 0.96 (dd, $J_{\text{H-H}} = 7.0$ Hz, $J_{\text{H-P}} = 11.9$ Hz, 12H). ¹³C{¹H} NMR (CD_2Cl_2 , 151 MHz, 22°C): δ (in ppm) = 139.0 (d, $J_{\text{C-P}} = 22.0$ Hz, C_q, 2C), 133.5 (d, $J_{\text{C-P}} = 2.8$ Hz, CH, 2C), 133.3 (d, $J_{\text{C-P}} = 4.5$ Hz, CH, 2C), 131.1 (d, $J_{\text{C-P}} = 28.0$ Hz, C_q, 2C), 128.8 (s, CH, 2C), 127.9 (d, $J_{\text{C-P}} = 1.6$ Hz, CH, 2C), 95.2 (dd, $J_{\text{C-P}} = 7.0$ Hz, $J_{\text{C-P}} = 2.6$ Hz, C_q, 2C), 23.9 (d, $J_{\text{C-P}} = 13.8$ Hz, CH, 4C), 20.4 (d, $J_{\text{C-P}} = 18.4$ Hz, CH₃, 4C), 19.7 (d, $J_{\text{C-P}} = 10.9$ Hz, CH₃, 4C). ³¹P{¹H} NMR (CD_2Cl_2 , 243 MHz, 22°C): δ (in ppm) = 4.9 (s). MS (LIFDI, toluene): Calcd. for $\text{C}_{26}\text{H}_{36}\text{P}_2$: 410.2292. Found: 410.2 [M]⁺. Anal. Calcd. for $\text{C}_{26}\text{H}_{36}\text{P}_2$ (410.52 g/mol): C 76.07, H 8.84. Found: C 75.89, H 9.25.



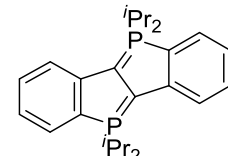
Synthesis of 5,5,10,10-tetraphenyl-5λ⁵,10λ⁵-phosphindolo[3,2-*b*]phosphindole (4a)

A solution of 1.0 eq **7a** (746 μmol, 408 mg) in 10 ml hexane and 5 ml toluene was stirred at 70°C for 5 d. The resulting precipitate was filtered off and washed with hexane. After drying in vacuum, analytically pure **4a** (332 mg, 607 μmol, 82%) was obtained as a black solid with a blue lustre (mp. 227°C). ¹H NMR (C_6D_6 , 600 MHz, 22°C): δ (in ppm) = 7.63–7.60 (m, 8H), 7.38–7.35 (m, 2H), 7.07–7.06 (m, 2H), 6.95–6.92 (m, 14H), 6.53–6.51 (m, 2H). ¹³C{¹H}, ³¹P NMR (toluene- d_8 , 151 MHz, 22°C): δ (in ppm) = 147.1 (C_q, 4C), 132.0 (CH, 8C), 131.0 (CH, 2C), 130.5 (CH, 4C), 130.0 (C_q, 2C), 128.9 (CH, 2C), 128.8 (CH, 8C), 117.6 (CH, 2C), 115.8 (CH, 2C), 110.8 (C_q, 2C), 67.6 (C=P, 2C). The signals at 128.9 and 128.8 (i.e. below the residual toluene signals) were identified in the DEPT NMR. ³¹P{¹H} NMR (toluene- d_8 , 162 MHz, -40°C): δ (in ppm) = -3.4 (s). MS (EI⁺): Calcd. for $\text{C}_{32}\text{H}_{23}\text{P}_2$: 469.1275. Found: 469.1 [M-Ph]⁺. Calcd. for $\text{C}_{38}\text{H}_{28}\text{P}_2$: 546.1666. Found: 546.2 [M]⁺. Anal. Calcd. for $\text{C}_{38}\text{H}_{28}\text{P}_2$ (546.59 g/mol): C 83.50, H 5.16. Found: C 83.21, H 5.37.



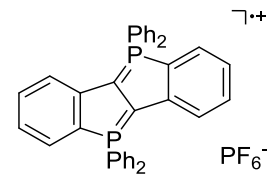
Synthesis of 5,5,10,10-tetraisopropyl-5λ⁵,10λ⁵-phosphindolo[3,2-*b*]phosphindole (4b)

A solution of 1.0 eq **7b** (244 μmol, 100 mg) in 10 ml hexane was stirred at 50°C for 4 d. The resulting precipitate was filtered off and washed with cold pentane. After drying in vacuum, analytically pure **4b** (71.3 mg, 172 μmol, 71%) was obtained in form of black-violet plates with a metallic lustre (mp. 147°C). ¹H NMR (toluene- d_8 , 400 MHz, -80°C): δ (in ppm) = 7.02–6.91 (m, 4H), 6.73–6.66 (m, 2H), 6.48–6.41 (m, 2H), 1.96–1.84 (m, 4H), 0.96–0.80 (m, 24H). ¹³C{¹H} NMR (toluene- d_8 , 101 MHz, -80°C): δ (in ppm) = 148.7 (t, $J_{\text{C-P}} = 15.6$ Hz, C_q, 2C), 132.1 (s, CH, 2C), 128.6–128.8 (m, CH, 2C), 118.0 (s, CH, 2C), 111.9 (s, CH, 2C), 105.0–106.2 (m, C_q, 2C), 62.9–64.3 (s, C=P, 2C), 25.2–25.8 (s, CH, 4C), 17.1 (d, $J_{\text{C-P}} = 6.1$ Hz, CH₃, 8C). ³¹P{¹H} NMR (toluene- d_8 , 161 MHz, -80°C): δ (in ppm) = 24.2 (s). MS (LIFDI, toluene): Calcd. for $\text{C}_{26}\text{H}_{36}\text{P}_2$: 410.2292. Found: 410.15 [M]⁺. Anal. Calcd. for $\text{C}_{26}\text{H}_{36}\text{P}_2$ (410.52 g/mol): C 76.07, H 8.84. Found: C 75.72, H 8.91.



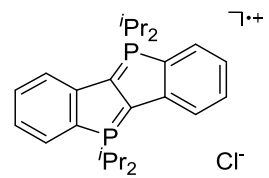
Synthesis of the 5,5,10,10-tetraphenyl-5λ⁵,10λ⁵-phosphindolo[3,2-*b*]phosphindolyl radical cation as its hexafluorophosphate salt (5a)

To a solution of 1.0 eq **4a** (366 μmol, 200 mg) in 12 ml THF 1.0 eq trityl hexafluorophosphate (366 μmol, 142 mg) was added. After stirring for 2.5 h at room temperature the reaction mixture was filtered. The precipitate was washed with THF and dried *in vacuo*. **5a** (158 mg, 228 μmol, 62%) was obtained as a deep blue-green solid (mp. 249°C dec.). ESR ($v = 9.634918$ GHz, DCM, 6 K): $g_e = 2.002$. HR-MS (ESI⁺): Calcd. for $\text{C}_{38}\text{H}_{29}\text{P}_2^+$: 547.1739. Found: 547.1745 [M]⁺. Anal. Calcd. for $\text{C}_{38}\text{H}_{28}\text{F}_6\text{P}_3$ (691.55 g/mol): C, 66.00; H, 4.08. Found: C 65.02, H 4.21.



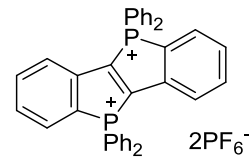
Synthesis of the 5,5,10,10-tetraisopropyl-5λ⁵,10λ⁵-phosphindolo[3,2-*b*]phosphindolyl radical cation as its chloride salt (5b)

To a solution of 1.0 eq **4b** (122 μmol, 50.0 mg) in 8 ml THF 1.0 eq trityl chloride (122 μmol, 34.0 mg) was added. After stirring for 1 h at room temperature the reaction mixture was filtered. The precipitate was washed with toluene (2 x 2 ml) and THF (1 x 1 ml) and dried *in vacuo*. **5b** (49.0 mg, 110 μmol, 90%) was obtained as a deep green solid (mp. 168°C). ESR ($v = 9.444930$ GHz, DCM, 22°C): $g_e = 2.002$, $A_{\text{iso}}(^{31}\text{P}) = 21.0$ G. HR-MS (ESI⁺): Calcd. for $\text{C}_{26}\text{H}_{36}\text{P}_2^+$: 410.2287. Found: 410.2288 [M]⁺. Anal. Calcd. for $\text{C}_{26}\text{H}_{36}\text{ClP}_2$ (445.97 g/mol): C 70.02, H 8.14. Found: C 69.78, H 7.57.



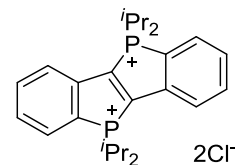
Synthesis of the 5,5,10,10-tetraphenyl-5 λ^5 ,10 λ^5 -phosphindolo[3,2-b]phosphindoldiyi dication as its bis-hexafluorophosphate salt (6a)

To a stirred solution of 1.0 eq **5a** (86.7 μmol , 60.0 mg) in 7 ml DCM was added 1.05 eq ferrocenium hexafluorophosphate (91.1 μmol , 30.2 mg) and the reaction mixture was stirred for 3 h at room temperature. The resulting precipitate was filtered off, washed with DCM and dried in vacuum to afford **6a** (38.0 mg, 45.4 μmol , 69%) as a fine yellow powder (mp. 280°C dec.). ^1H NMR (CD_3CN , 400 MHz, -40°C): δ (in ppm) = 8.28-8.23 (m, 2H), 8.04-7.97 (m, 12H), 7.90-7.86 (m, 2H), 7.83-7.81 (m, 2H), 7.77-7.74 (m, 10H). $^{13}\text{C}\{\text{H}, \text{P}\}$ NMR (CD_3CN , 75 MHz, 25°C): δ (in ppm) = 148.3 (C_{q} , 2C), 138.8 (C_{q} , 4C), 138.8 (CH, 4C), 138.6 (CH, 2C), 136.1 (CH, 8C), 135.5 (CH, 2C), 134.6 (CH, 2C), 132.6 (CH, 8C), 128.8 (CH, 2C), 126.3 (C_{q} , 2C), 113.6 (C_{q} , 2C). $^{31}\text{P}\{\text{H}\}$ NMR (CD_3CN , 162 MHz, -40°C): δ (in ppm) = 25.8 (s), -144.8 (sept, $J_{\text{P-F}} = 706.9$ Hz). HR-MS (ESI $^+$): Calcd. for $\text{C}_{38}\text{H}_{28}\text{OP}_2$: 536.1688. Found: 536.1689 [M+OH] $^+$. Anal. Calcd. for $\text{C}_{38}\text{H}_{28}\text{F}_{12}\text{P}_4$ (836.10 g/mol): C 54.56, H 3.37. Found: C 53.44 H 3.64.



Synthesis of the 5,5,10,10-tetraisopropyl-5 λ^5 ,10 λ^5 -phosphindolo[3,2-b]phosphindoldiyi dication as its dichloride salt (6b)

To a solution of 1.0 eq **5b** (110 μmol , 50.0 mg) in 5 ml DCM was added 0.5 eq iodobenzene dichloride (60.5 μmol , 16.6 mg) and the reaction mixture was stirred for 1 h at room temperature. The resulting precipitate was collected on a sinter glass frit, washed with DCM and dried in vacuum to afford **6b** (36.6 mg, 69%) as a fine yellow powder (mp. 247-253°C). ^1H NMR (D_2O , 600 MHz, 22°C): δ (in ppm) = 8.27-8.18 (m, 2H), 8.05-7.98 (m, 2H), 7.98-7.93 (m, 2H), 7.90-7.82 (m, 2H), 3.75-3.60 (m, 4H), 1.50-1.30 (m, 24H). $^{13}\text{C}\{\text{H}, \text{P}\}$ NMR (D_2O , 75 MHz, 25°C): δ (in ppm) = 146.6 (C_{q} , 2C), 138.6 (C_{q} , 2C), 137.0 (CH, 2C), 134.2 (CH, 2C), 132.6 (CH, 2C), 127.4 (CH, 2C), 120.0 (C_{q} , 2C), 22.5 (CH, 4C), 15.3 (CH₃, 4C), 14.8 (CH₃, 4C). $^{31}\text{P}\{\text{H}\}$ NMR (D_2O , 243 MHz, 22°C): δ (in ppm) = 58.5 (s). HR-MS (ESI $^+$): Calcd. for $\text{C}_{26}\text{H}_{37}\text{OP}_2^+$: 427.2314. Found: 427.2315 [M+OH] $^+$. Anal. Calcd. for $\text{C}_{26}\text{H}_{36}\text{Cl}_2\text{P}_2$ (481.42 g/mol): C 64.87, H 7.54. Found: C 64.15, H 7.46.



Selected NMR Spectra

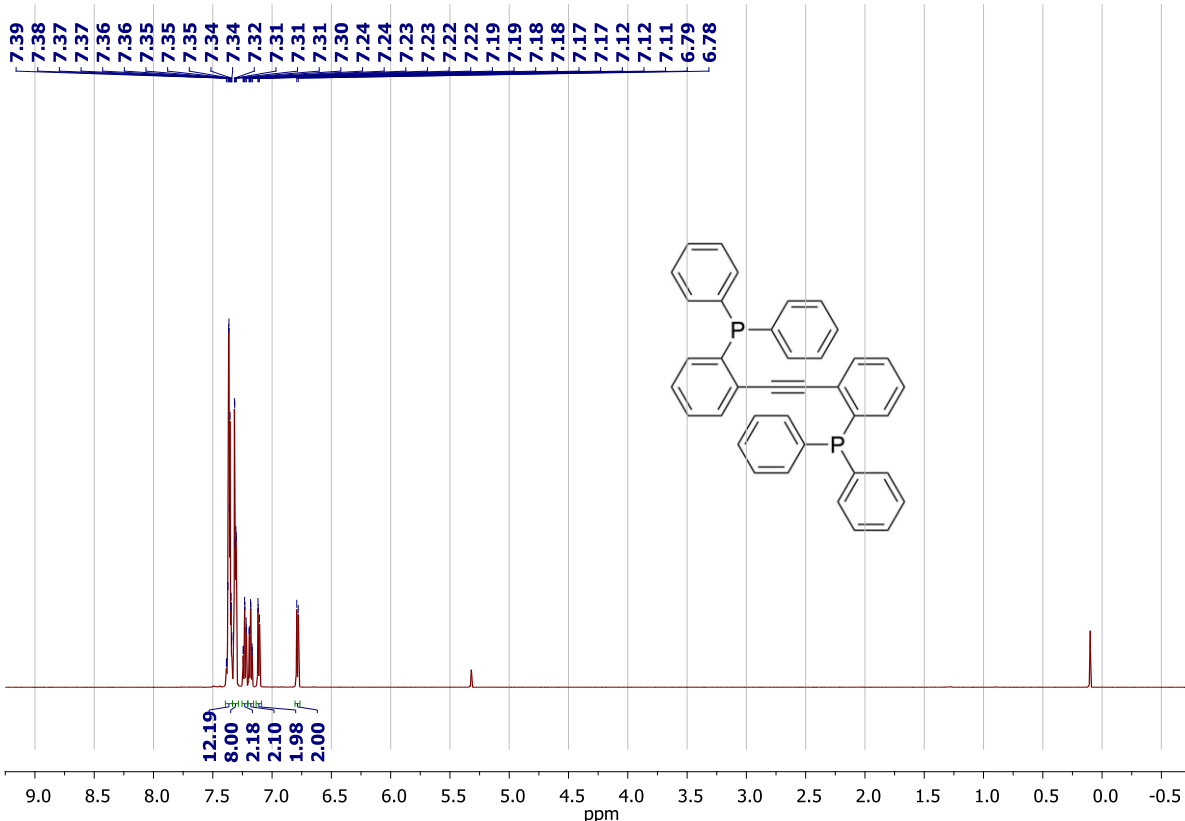


Figure S1. $^1\text{H}\{\text{P}\}$ NMR spectrum of **7a** (600 MHz, CD_2Cl_2 , 295 K).

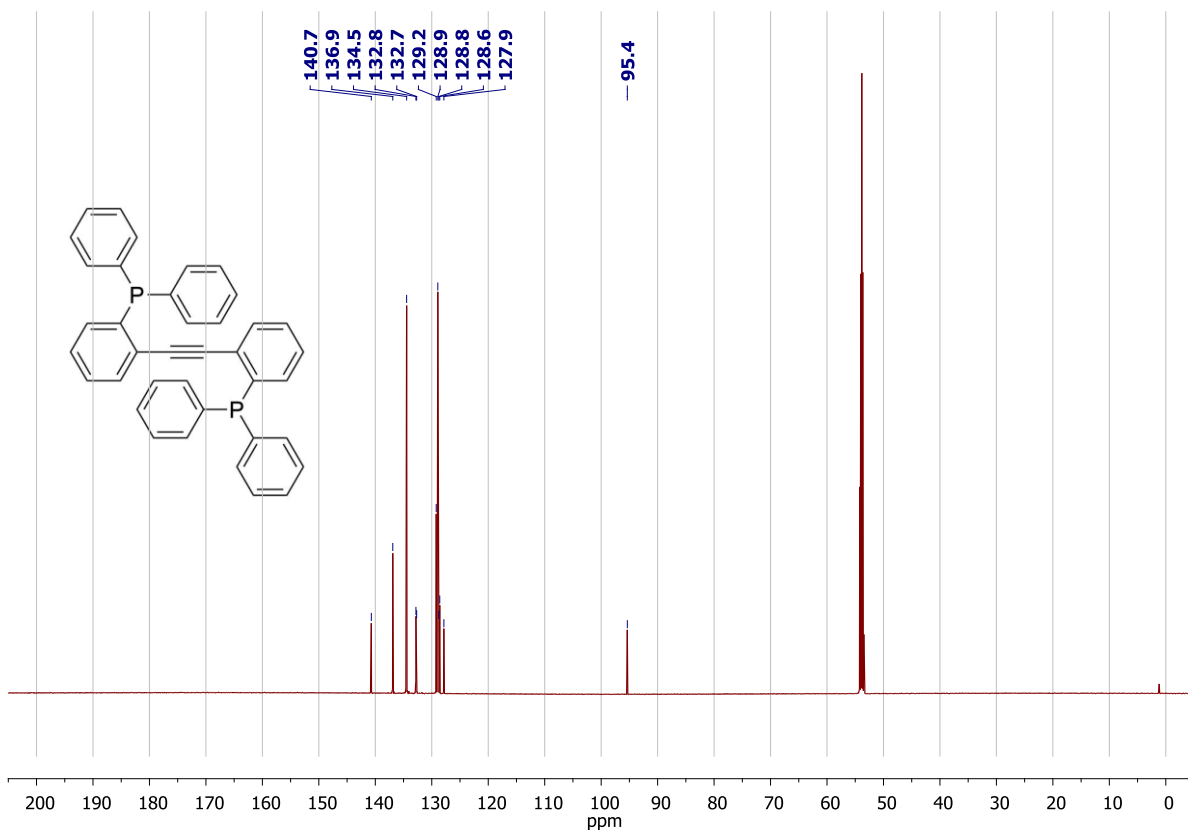


Figure S2. $^{13}\text{C}\{^{1}\text{H},^{31}\text{P}\}$ NMR spectrum of **7a** (151 MHz, CD_2Cl_2 , 295 K).

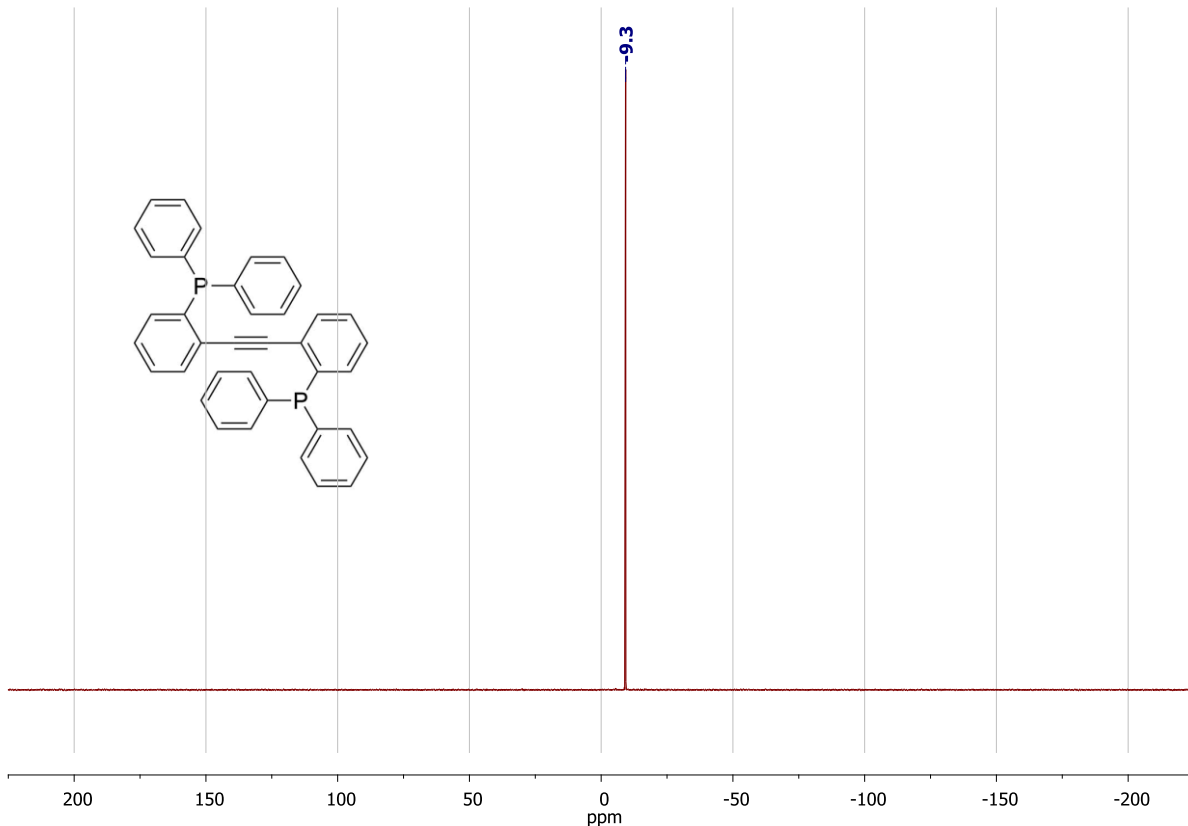


Figure S3. $^{31}\text{P}\{^{1}\text{H}\}$ NMR spectrum of **7a** (242 MHz, CD_2Cl_2 , 295 K).

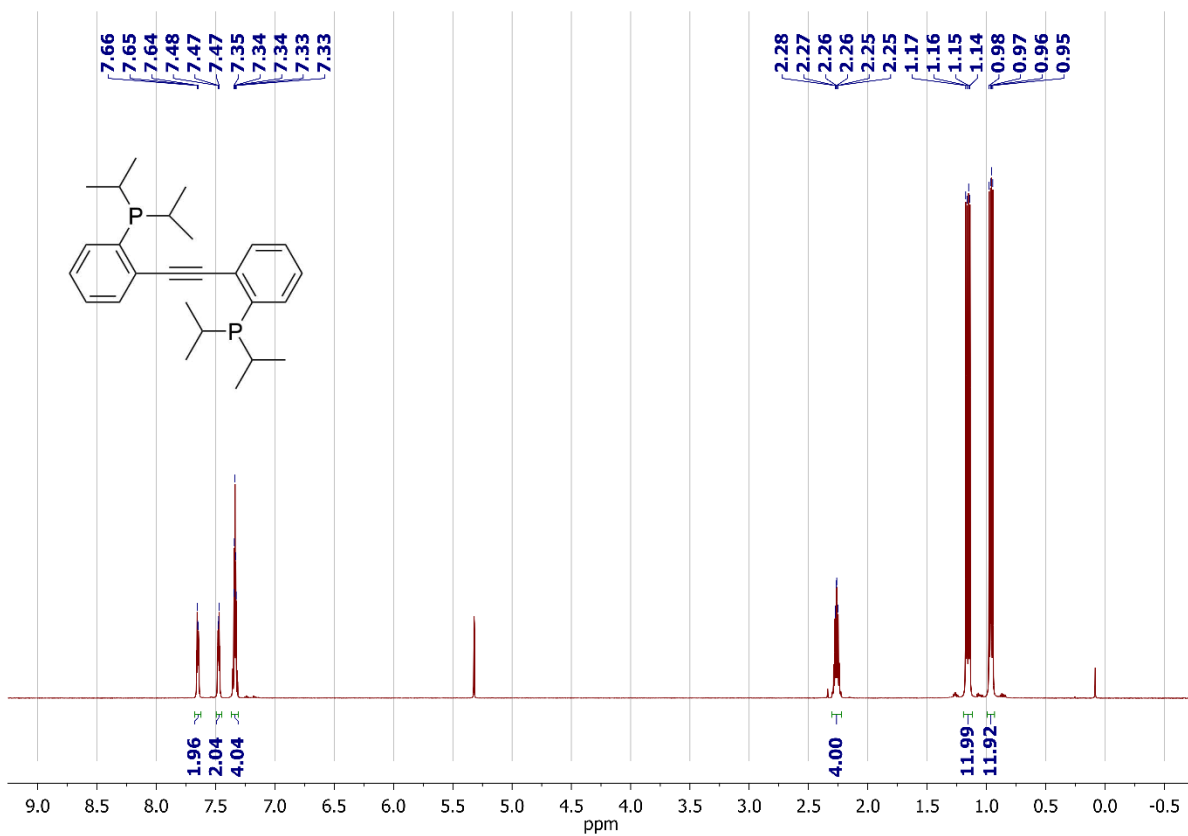


Figure S4. ^1H NMR spectrum of **7b** (600 MHz, CD_2Cl_2 , 295 K).

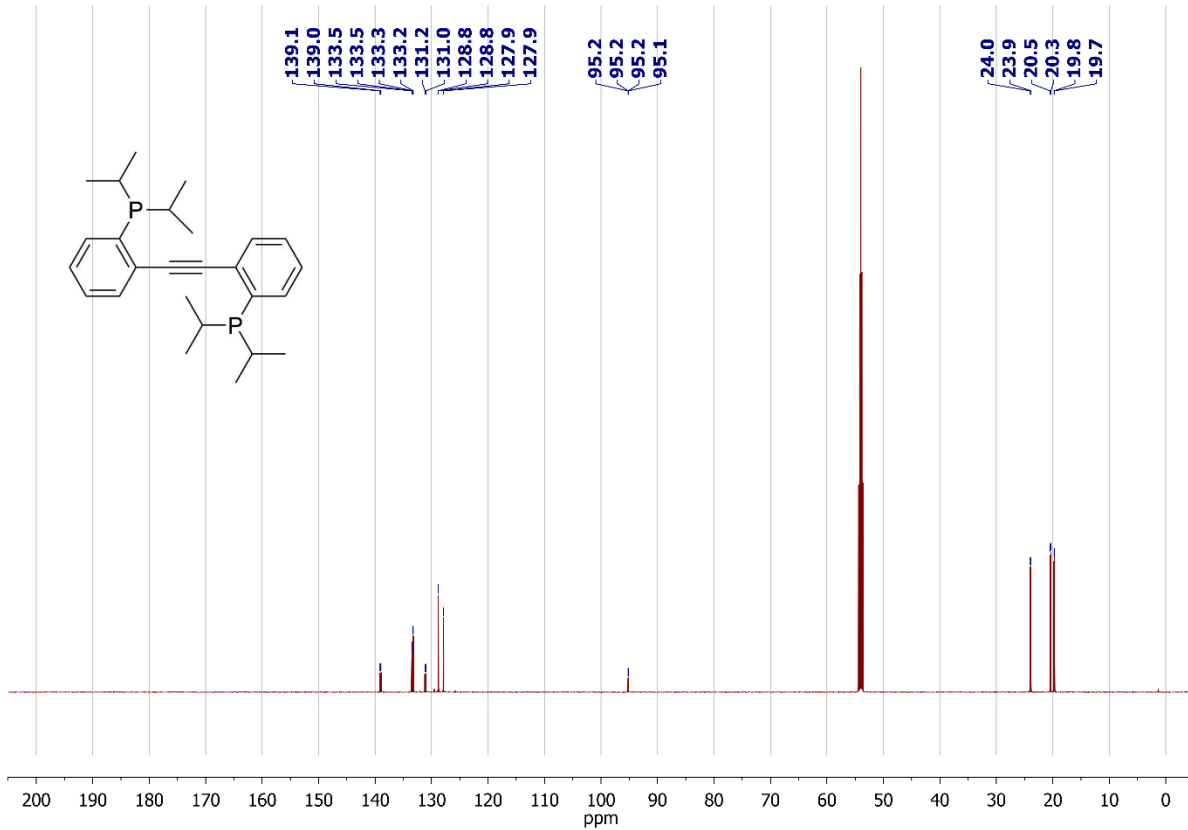


Figure S5. $^{13}\text{C}\{^1\text{H}\}$ NMR spectrum of **7b** (151 MHz, CD_2Cl_2 , 295 K).

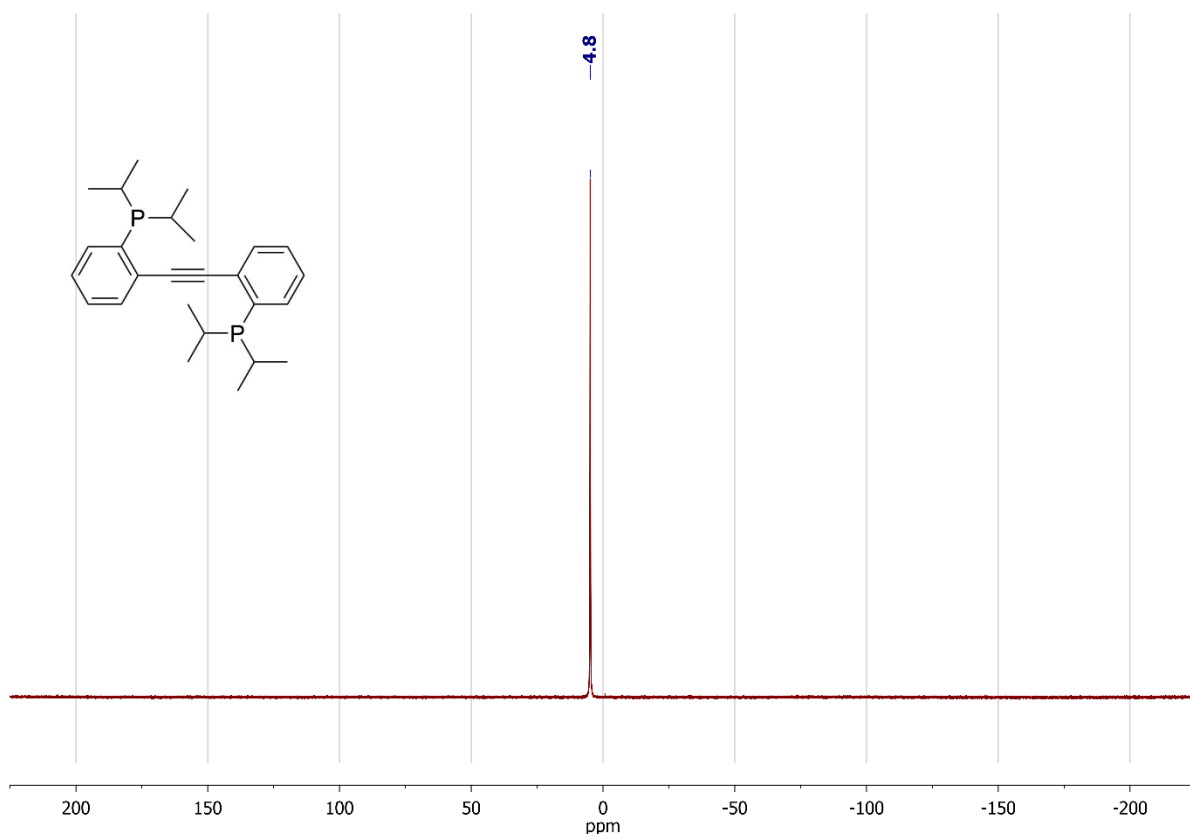


Figure S6. $^{31}\text{P}\{\text{H}\}$ NMR spectrum of **7b** (243 MHz, CD_2Cl_2 , 295 K).

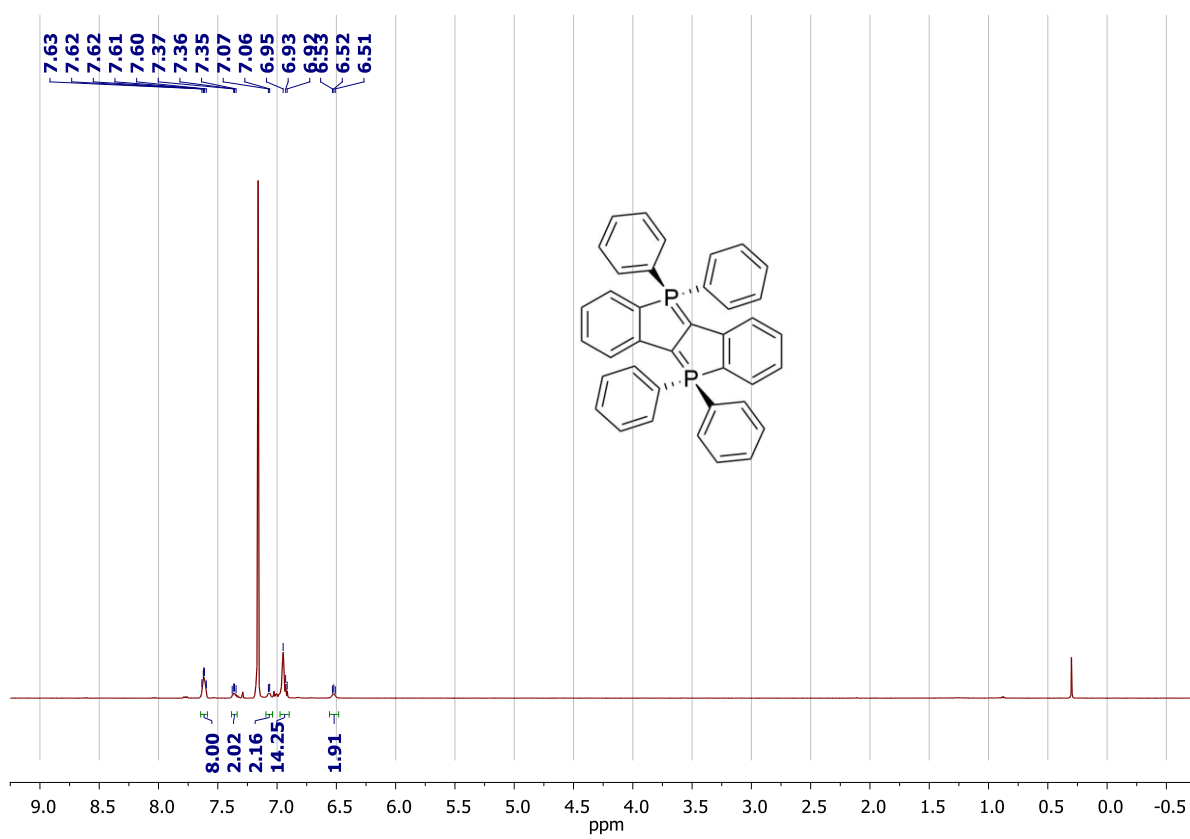


Figure S7. ^1H NMR spectrum of **4a** (600 MHz, C_6D_6 , 295 K). Due to the low solubility of **4a** in benzene (or toluene), the residual solvent appears as a dominant signal in the ^1H NMR spectrum.

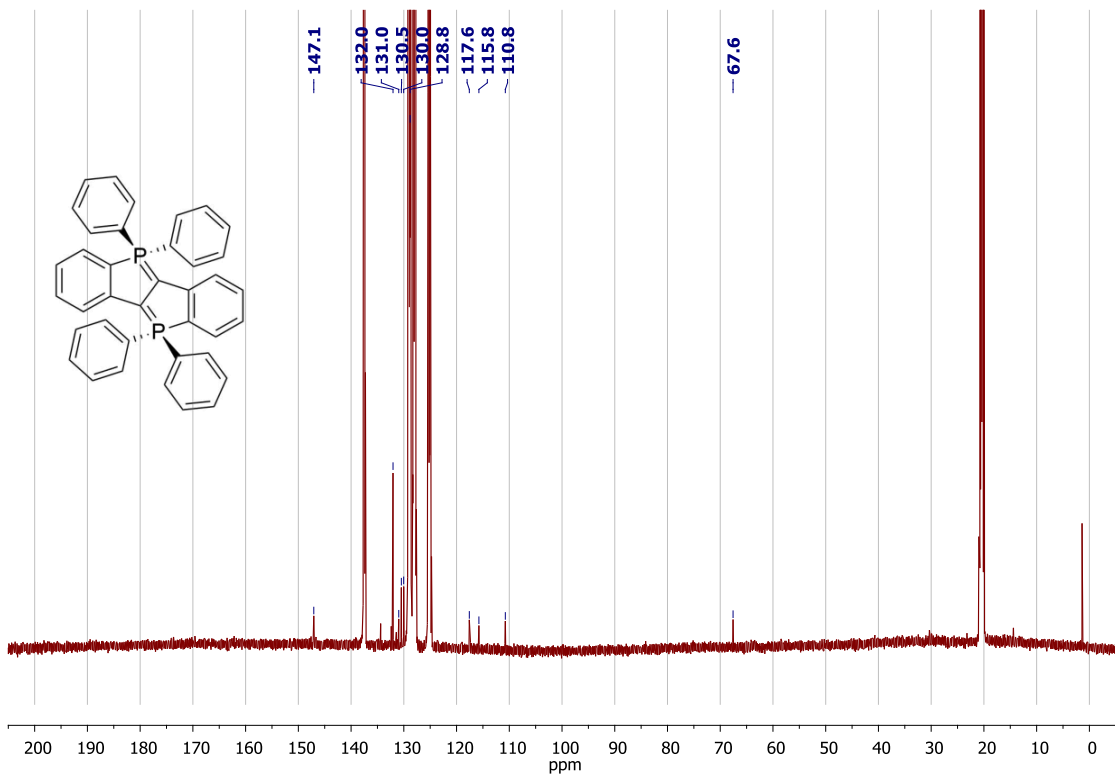


Figure S8. $^{13}\text{C}\{^1\text{H}, ^{31}\text{P}\}$ NMR spectrum of **4a** (151 MHz, toluene- d_8 , 295 K). Due to the low solubility of **4a** in toluene, the residual solvent signals appear as dominant signals in the shown NMR spectrum. In THF- d_8 or CD_2Cl_2 , decomposition is too fast to allow for the acquisition of carbon NMR spectra.

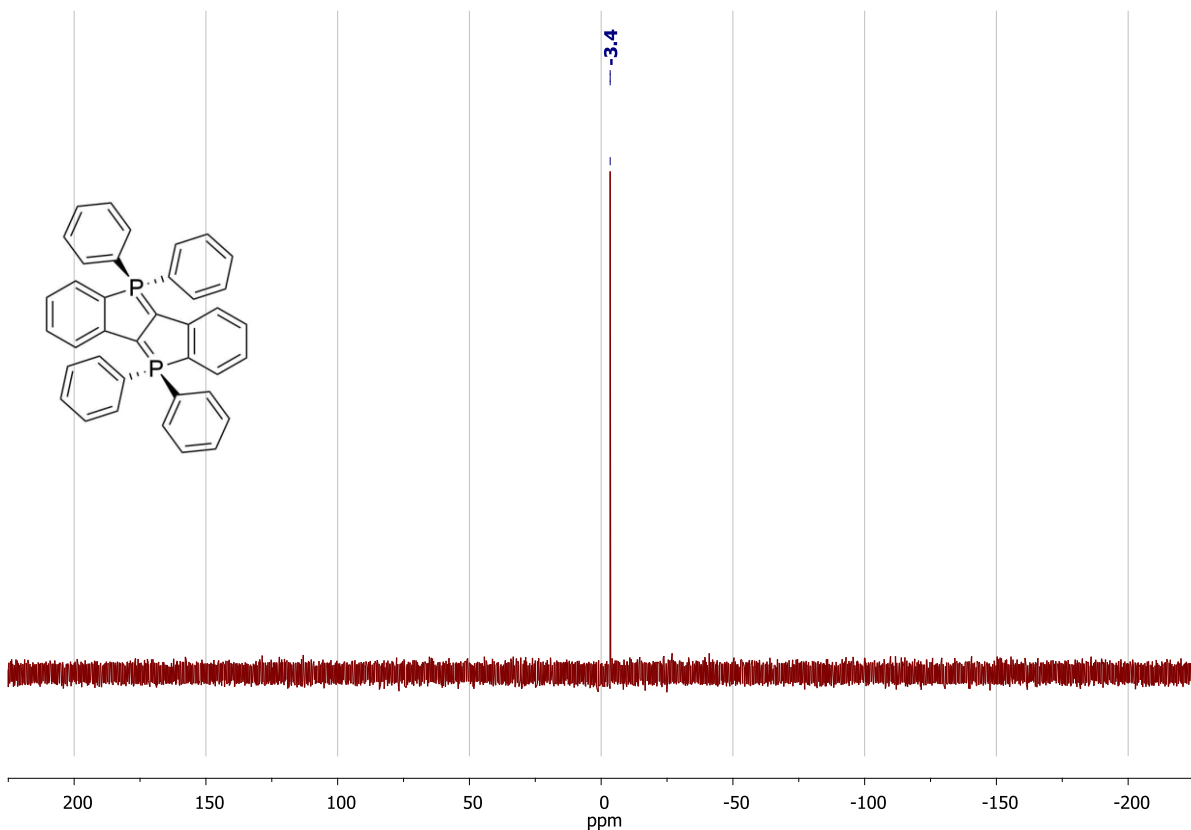


Figure S9. $^{31}\text{P}\{^1\text{H}\}$ NMR spectrum of **4a** (162 MHz, toluene- d_8 , 233 K). Due to the low solubility of **4a** in toluene (i.e. the presence of undissolved compound in the NMR tube), a significantly broadened singlet ^{31}P NMR signal is observed at room temperature.

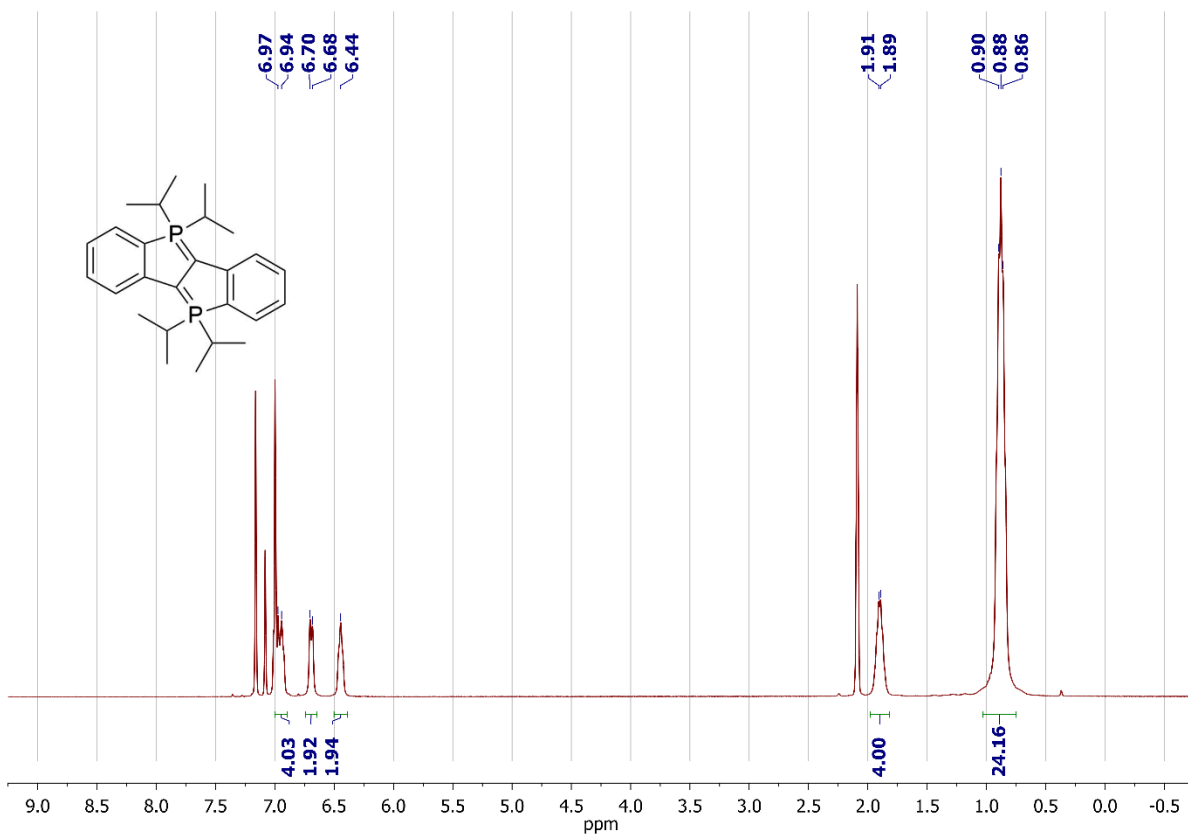


Figure S10. ^1H NMR spectrum of **4b** (400 MHz, toluene- d_8 , 193 K).

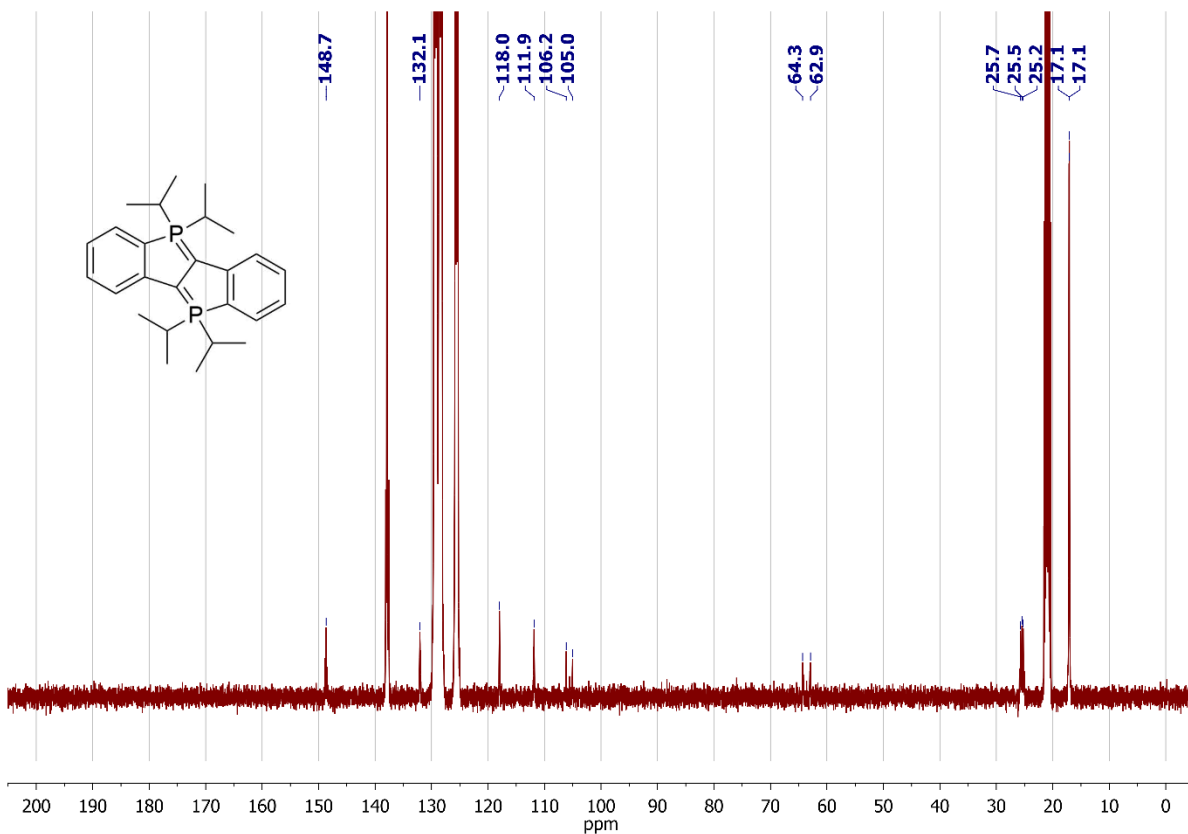


Figure S11. $^{13}\text{C}\{^1\text{H}\}$ NMR spectrum of **4b** (101 MHz, toluene- d_8 , 193 K).

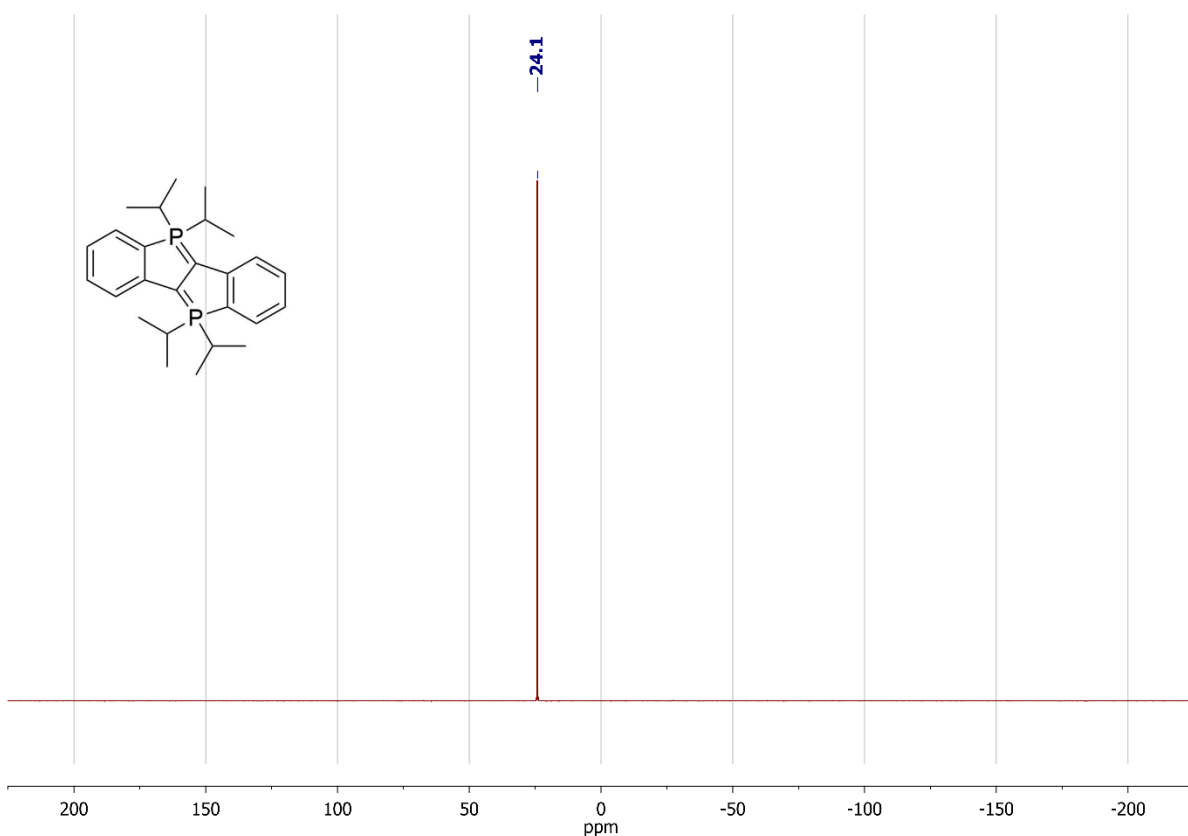


Figure S12. $^{31}\text{P}\{^1\text{H}\}$ NMR spectrum of **4b** (161 MHz, toluene- d_6 , 193 K).

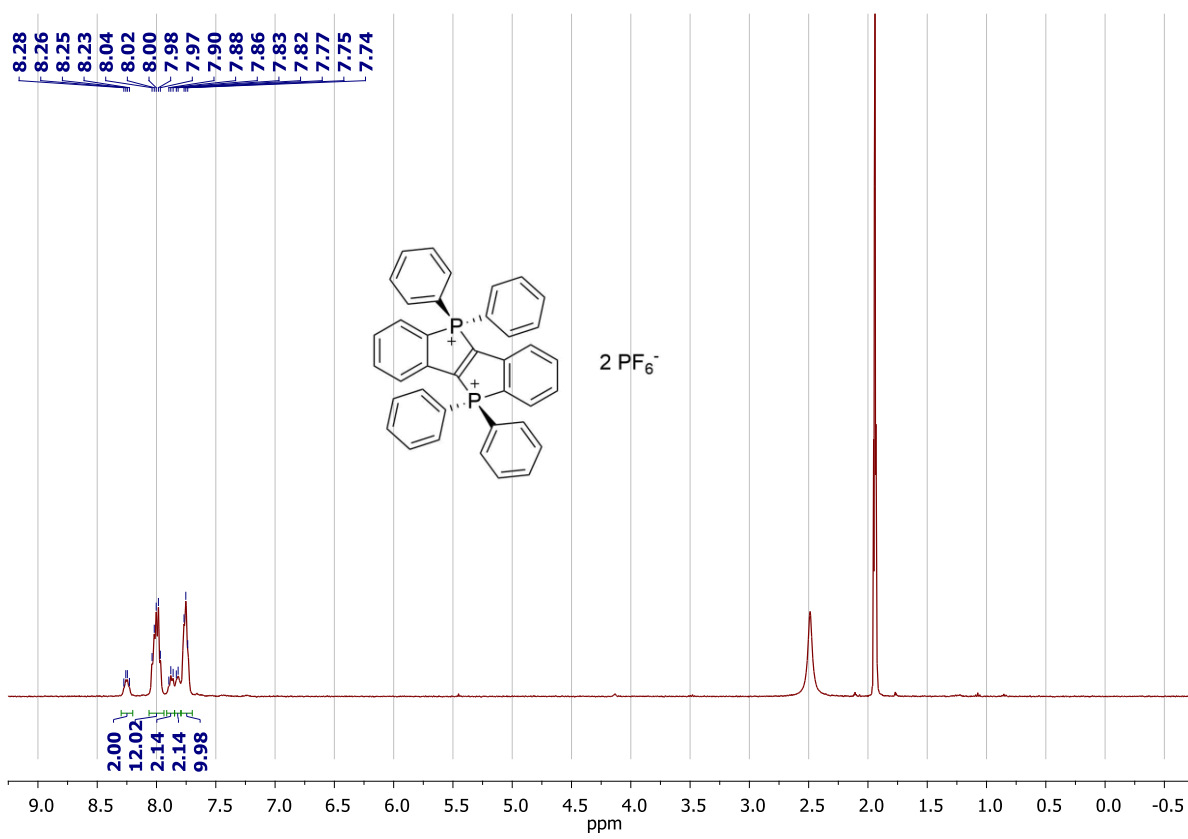


Figure S13. ^1H NMR spectrum of **6a** (400 MHz, CD₃CN, 233 K). Deuterated acetonitrile was used as received, i.e. the broad signal at 2.5 ppm corresponds to residual water present in the solvent.

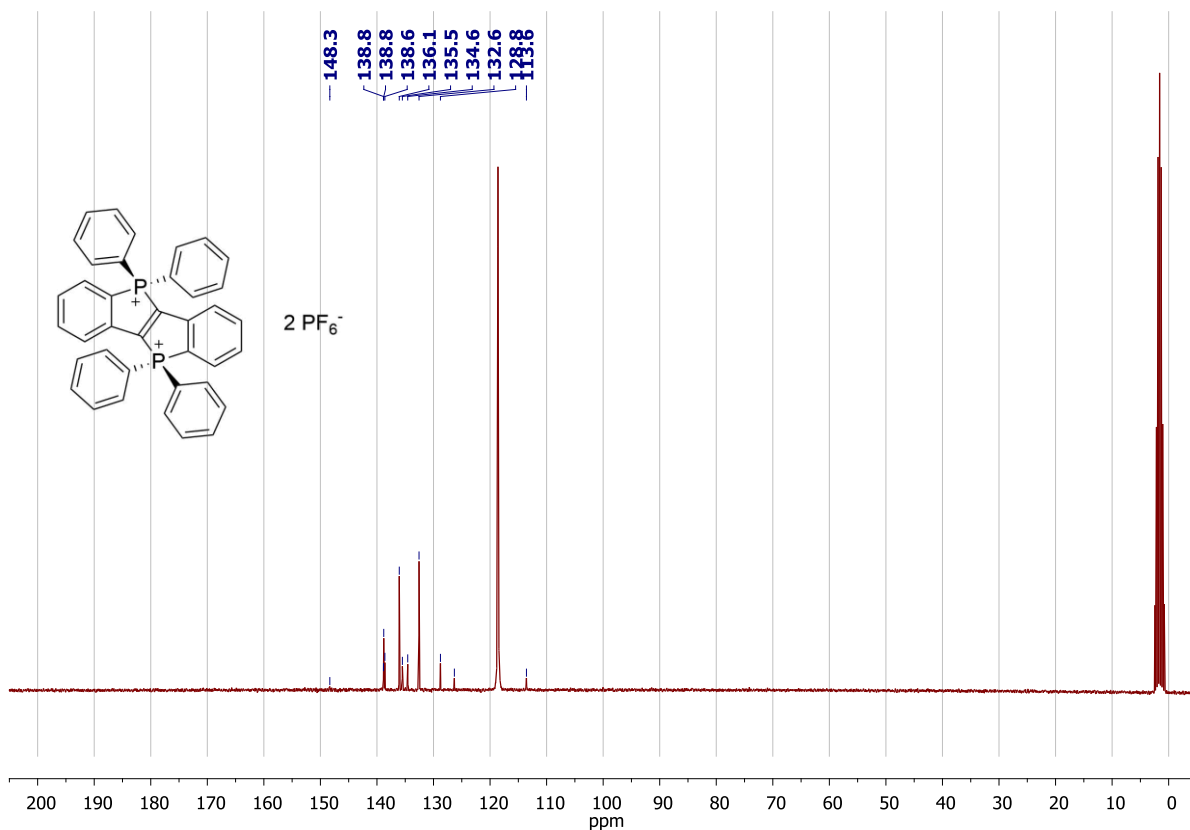


Figure S14. $^{13}\text{C}\{^{1}\text{H}, ^{31}\text{P}\}$ NMR spectrum of **6a** (75 MHz, CD_3CN , 298 K).

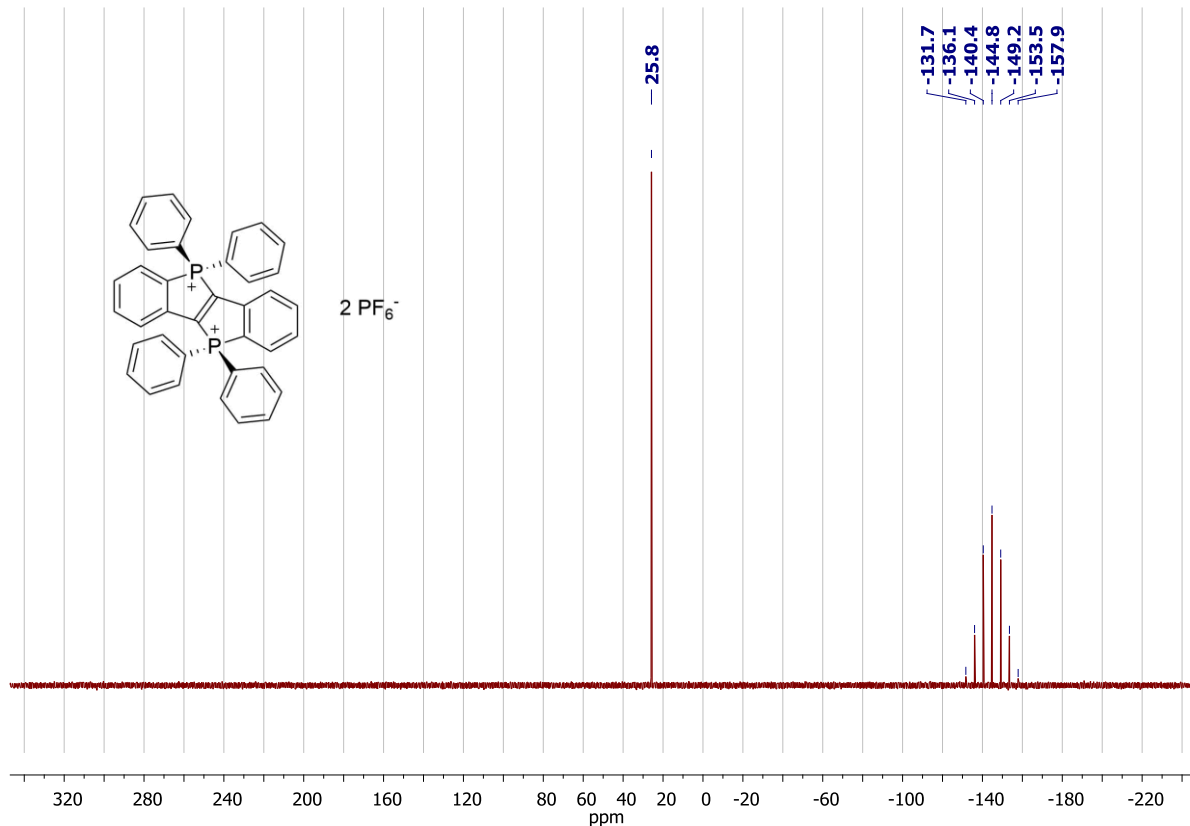


Figure S15. $^{31}\text{P}\{^{1}\text{H}\}$ NMR spectrum of **6a** (162 MHz, CD_3CN , 233 K).

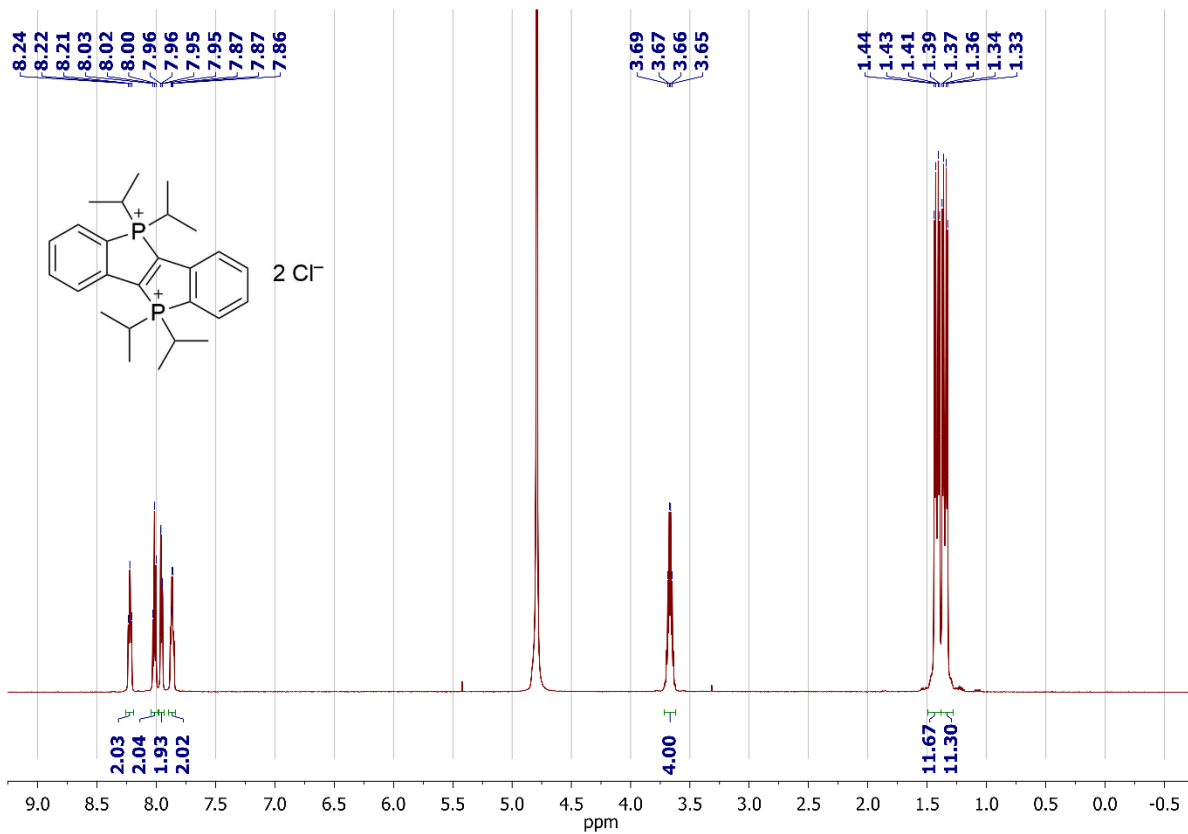


Figure S16. ^1H NMR spectrum of **6b** (600 MHz, D_2O , 295 K).

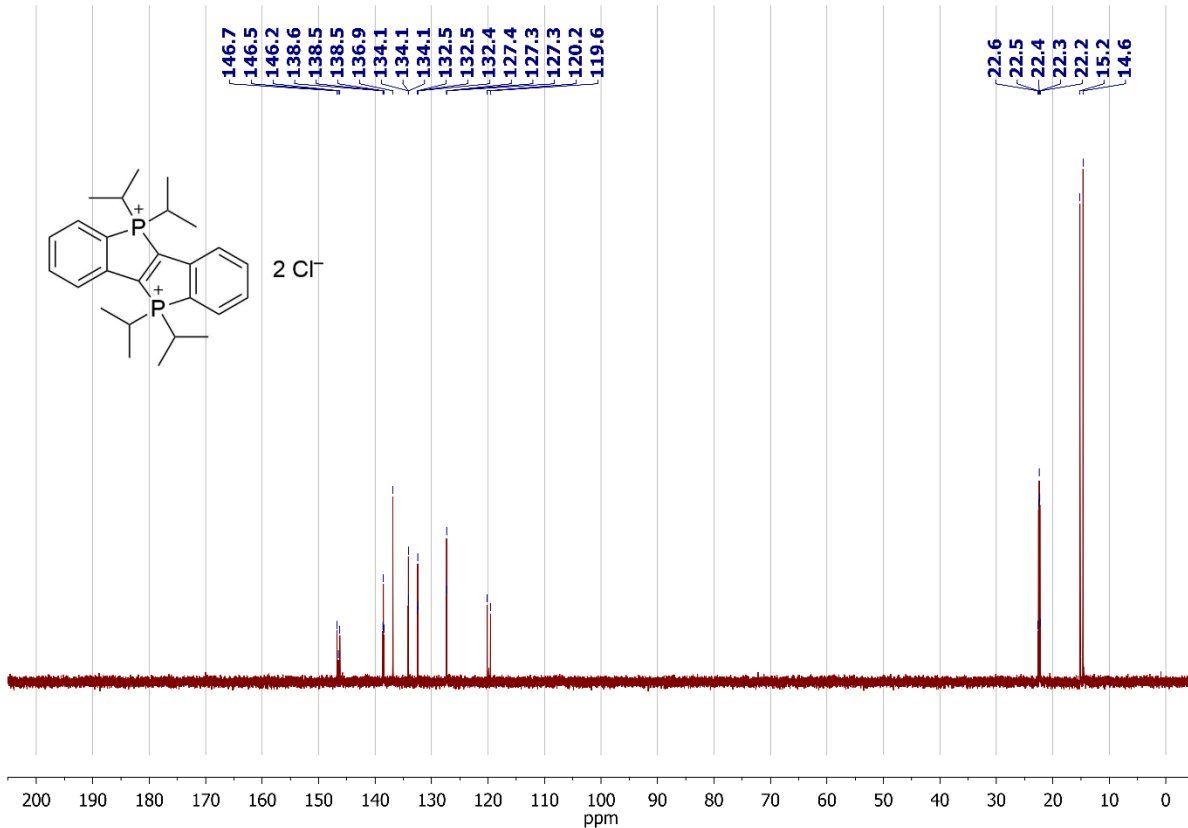


Figure S17. $^{13}\text{C}\{^1\text{H}\}$ NMR spectrum of **6b** (151 MHz, D_2O , 295 K).

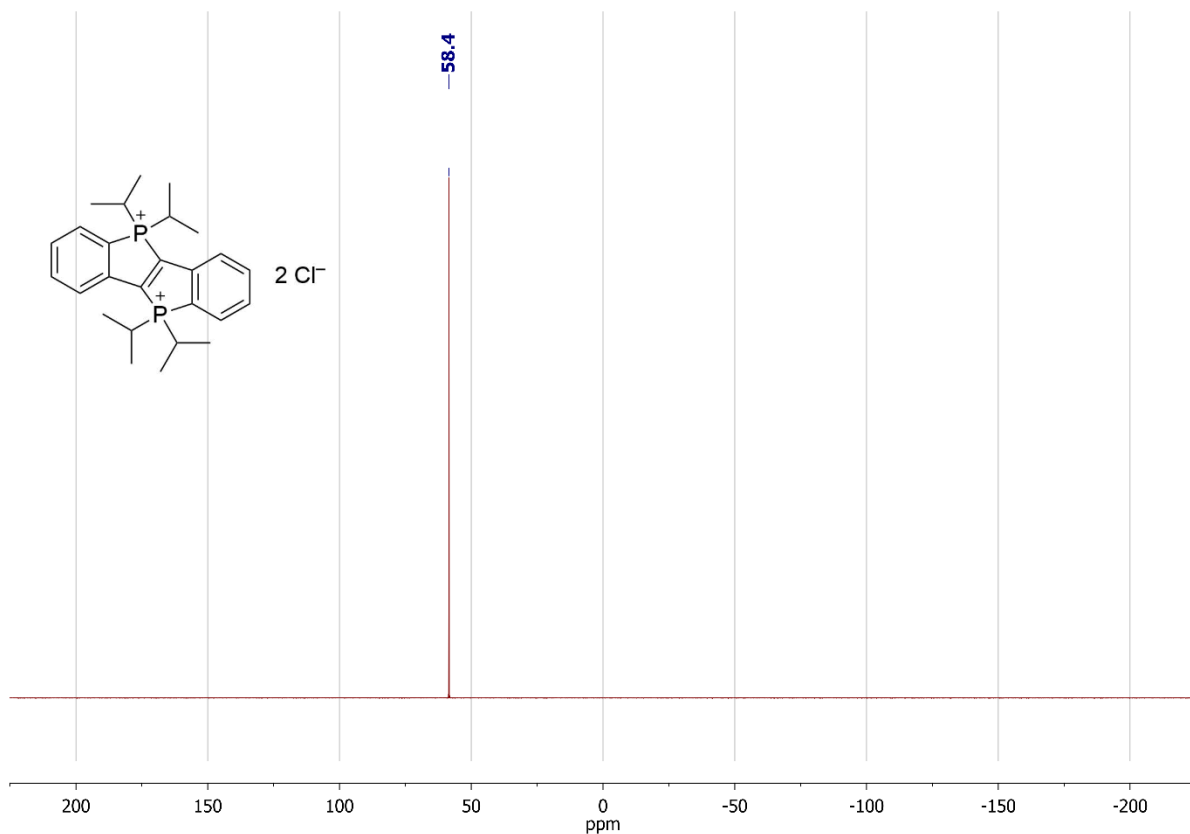


Figure S18. $^{31}\text{P}\{^1\text{H}\}$ NMR spectrum of **6b** (243 MHz, D₂O, 295 K).

Selected EPR Spectra and Spin Density Plots

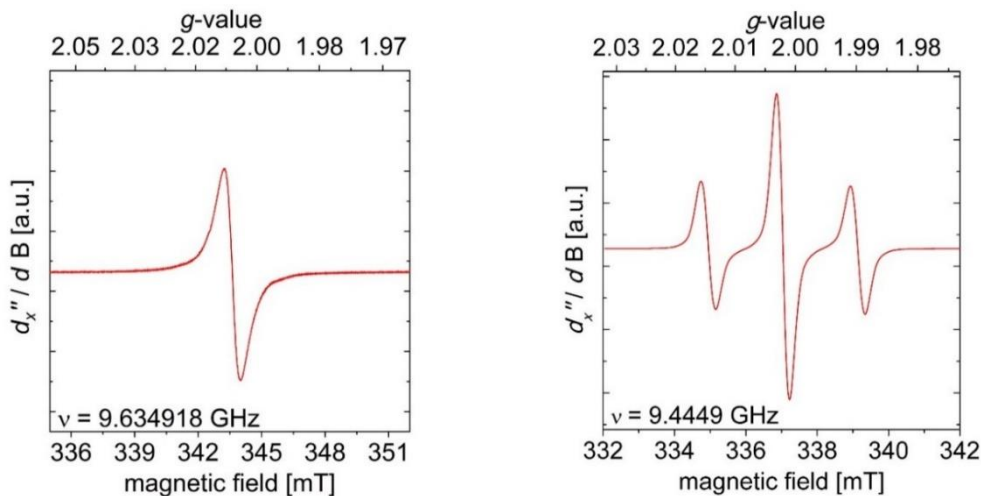


Figure S19. X-band EPR spectra of **5a** (6 K, recorded in frozen CH_2Cl_2 , a virtually identical spectrum was recorded at r.t.) and **5b** (r.t., recorded in CH_2Cl_2 , a virtually identical spectrum was recorded at 6 K). Independent of the temperature, coupling to the ^{31}P nuclei was only observed for **5b** ($A_0 = 21$ G). This result was reproduced with different samples from separate batches and in different solvents (CH_2Cl_2 and THF) and on different EPR spectrometers (Magnettech MiniScope MS400 and Bruker ESP 300 spectrometer). DFT calculations are indicative of lower Mulliken spin densities on the phosphorus atoms of **5a** in comparison to **5b** (c.f. Fig. S20 and S21), which is in line with the experimental findings (c.f. footnote 24 in the main article).

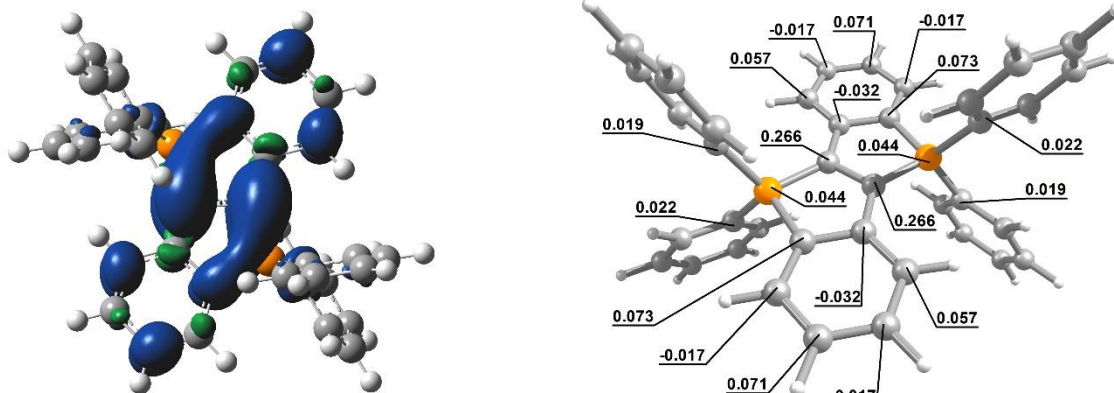


Figure S20. Spin density plot (isovalue = 0.001, Gaussian G09RevD.01, UB3LYP/def2-TZVPP) and Mulliken spin densities (values below a threshold of ± 0.01 omitted for clarity, ORCA 4.0, UB3LYP/EPR-III) of **5a** (details on DFT calculations are provided on page S17).

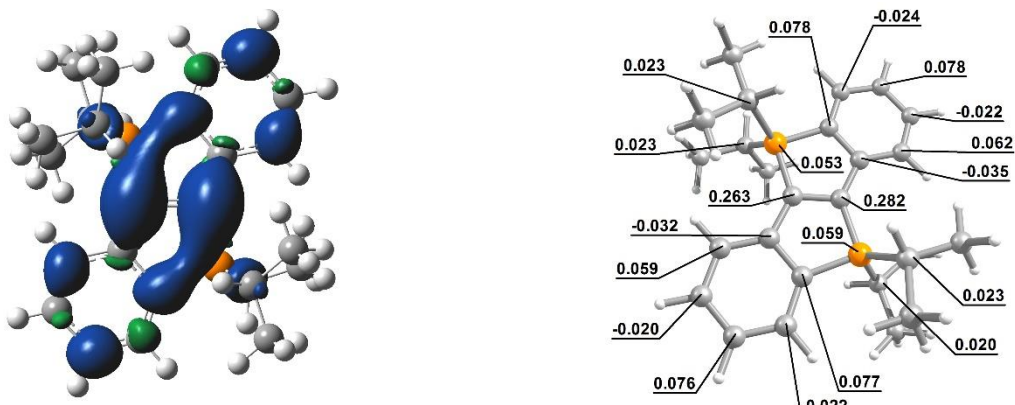


Figure S21. Spin density plot (isovalue = 0.001, Gaussian G09RevD.01, UB3LYP/def2-TZVPP) and Mulliken spin densities (values below a threshold of ± 0.01 omitted for clarity, ORCA 4.0, UB3LYP/EPR-III) of **5b** (details on DFT calculations are provided on page S17).

Photophysical Measurements

Sample Preparation. In a Glovebox, compounds **4a**, **4b**, **5a** and **5b** were dissolved in rigorously dried, freshly distilled solvents at known concentrations. These solutions were transferred to UV/Vis cells and the cells were carefully sealed (Teflon-valve) prior to removal from the Glovebox. Compounds **6a** and **6b** were freshly dissolved in pure water (spectroscopic grade, Sigma-Aldrich) and acetonitrile (HPLC grade, Honeywell) at known concentrations. UV/Vis absorption spectra were measured in 1 cm fused silica cells (Starna). For fluorescence measurements (**6a** and **6b**), the sample concentration was such that maximum absorption lies below 0.1 in a 1 cm cuvette.

Absorption Spectroscopy. Stationary UV-Vis absorption spectra were recorded on a Cary 5000 UV-Vis-NIR spectrophotometer (compounds **4a**, **4b**, **5a** and **5b**) or on a Shimadzu UV-2600 spectrophotometer (compounds **6a** and **6b**). Each spectrum was scanned five times and averaged. Spectra were baseline corrected.

Fluorescence Spectroscopy. Stationary fluorescence spectra were obtained at right angle geometry in JASCO FP-8200 spectrofluorometer. Excitation and emission spectra were measured five times and averaged. The slit width was 2.5 nm. Solvent baseline was measured in the same conditions and subtracted. The so-obtained fluorescence emission spectra were corrected for instrumental factors by the method described by Gardecki and Maroncelli.³ For this purpose, the emission spectra of Tryptophan (Sigma-Aldrich), TPB (TCI), α -NPO (Radiant Dyes Laser), Coumarin 153 (Radiant Dyes Laser), DCM (Sigma-Aldrich) and LDS 751 (Radiant Dyes Laser) were measured following the same procedure. The standard dyes were dissolved in the same spectroscopic grade solvents (Sigma-Aldrich) as in the original paper of Gardecki and Maroncelli. The correction function was validated by measuring the emission spectra of Quinine Sulfate and Fluorescein, with known fluorescence quantum distributions. Deviations are below 10%. Fluorescence quantum yields were determined relative to Quinine Sulfate (Sigma-Aldrich) in an aqueous 0.1 M H₂SO₄ solution, for which a fluorescence quantum yields of 0.546 was determined.⁴

Time-resolved fluorescence. Fluorescence lifetimes were measured by time-correlated single photon counting (TC-SPC) in a LifeSpec-II spectrofluorometer (Edinburgh Instruments). The sample was excited at 375 nm with an EPL-375 diode laser (pulse duration about 100 ps) working at 5 MHz repetition rate (Edinburgh Instruments). Fluorescence was collected at right angle and dispersed in a double subtractive monochromator. The emission maximum was selected as emission wavelength. Fluorescence decay curves were deconvoluted with the instrument response function measured with a scatterer. Fluorescence decay was found to be monoexponential for compounds **6a** and **6b**.

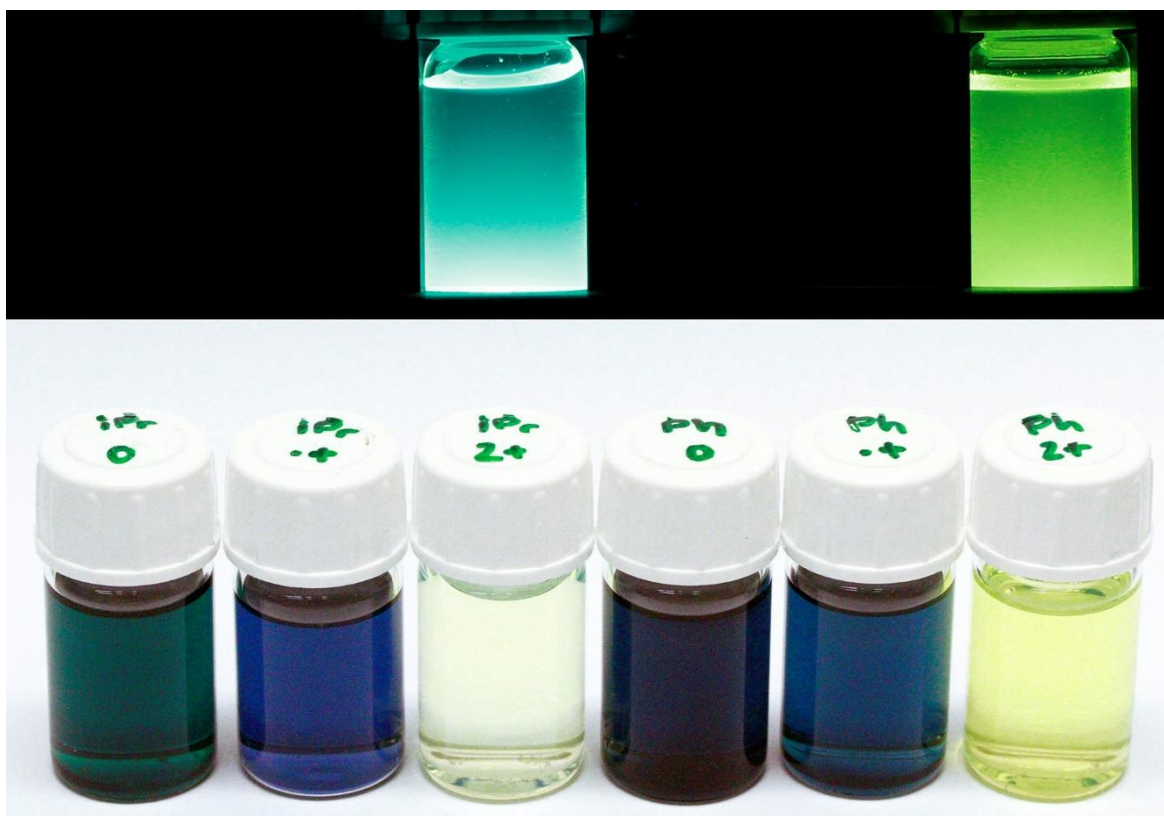


Figure S22. Photographs of **4b**, **5b**, **6b** and **4a**, **5a**, **6a** (from left to right) in solution under UV-light (top) and daylight (bottom).

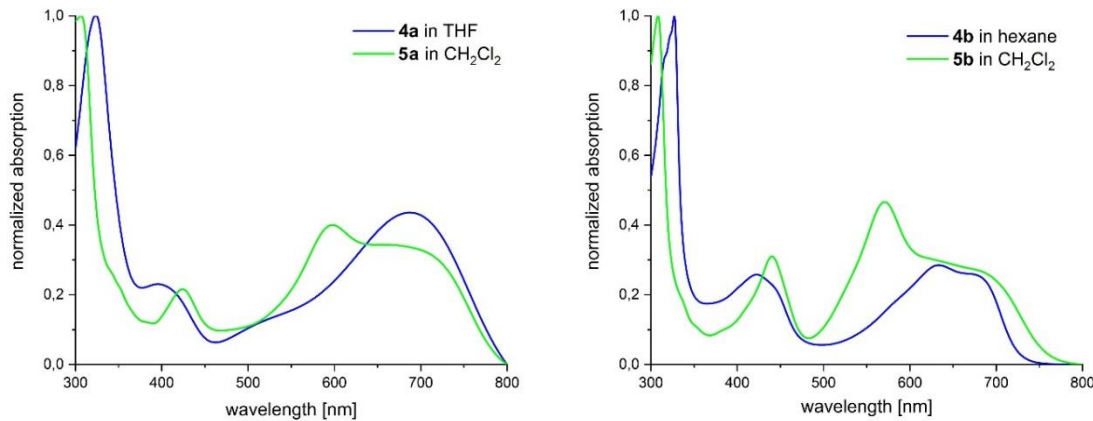


Figure S23. UV/Vis absorption spectra of **4a**, **4b**, **5a** and **5b**.

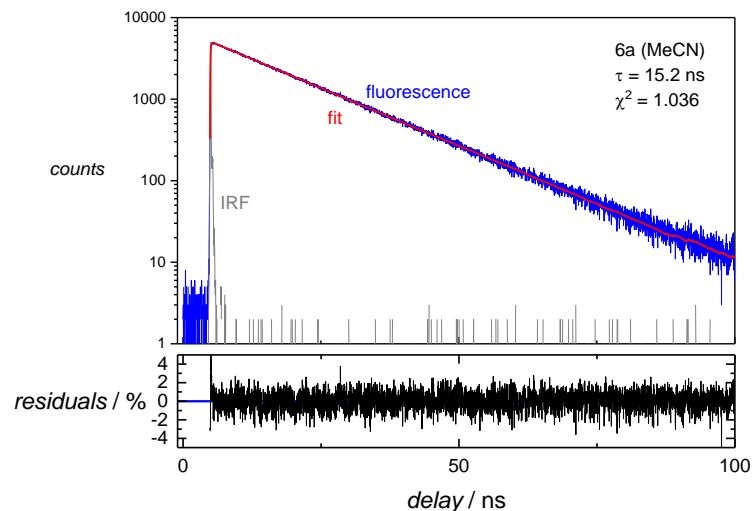


Figure S24. Fluorescence decay curve of **6a** in acetonitrile monitored at 511 nm under excitation at 375 nm. A monoexponential response function was convoluted with the instrument response function (IRF, gray) and fitted (red). The fitting parameters are indicated in the inset. The lower panel shows the weighted residuals for the fit.

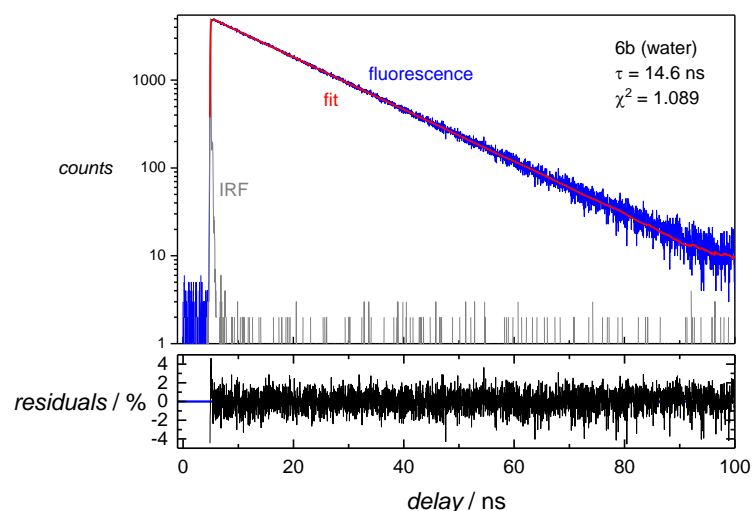


Figure S25. Fluorescence decay curve of **6b** in water monitored at 481 nm under excitation at 375 nm. A monoexponential response function was convoluted with the instrument response function (IRF, gray) and fitted (red). The fitting parameters are indicated in the inset. The lower panel shows the weighted residuals for the fit.

Details on DFT Calculations

DFT calculations were performed with the Gaussian 09 program suite (G09RevB.01 incl. NBO 5.9 or G09RevD.01)⁵ using the B3LYP hybrid functional.⁶ Geometry optimizations were carried out without symmetry restrictions and the stationary point were identified as minima by analytical frequency analysis. In the case of ground state calculations, all atoms were described with the def2-TZVPP basis set.⁷ Grimme's dispersion correction (DFT-D3)⁸ was applied as implemented in Gaussian. Mulliken spin densities for **5a** and **5b** were calculated with the ORCA 4.0 program suite using the UB3LYP/functional and the EPR-III basis set as implemented in ORCA.⁹ Plots of the optimized molecular structures of **4a**, **4b**, **5a**, **5b**, **6a** and **6b** and xyz-coordinates for the optimized geometries of **7a**, **7b**, **4a**, **4b**, **5a**, **5b**, **6a** and **6b** are provided below.

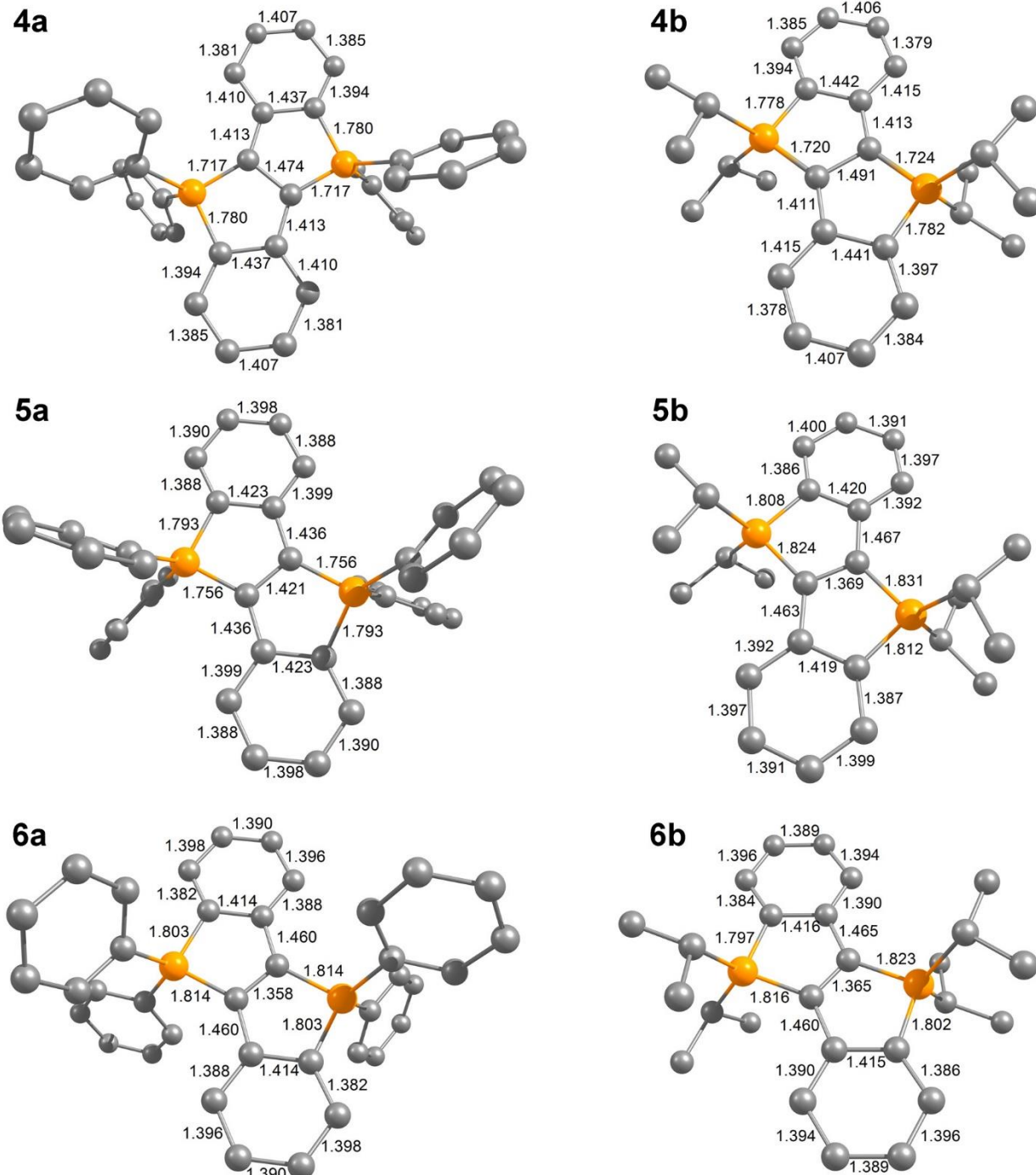


Figure S26. Optimized molecular structures of **4a**, **4b**, **5a**, **5b**, **6a** and **6b** (incl. selected bond lengths of the respective core skeletons).

Table S1. Optimized coordinates for **7a** (charge = 0, multiplicity = 1).

Label	Symbol	X	Y	Z
1	C	-1.59264000	2.05628000	0.57339000
2	C	-0.55179000	1.49504000	1.36364000
3	C	0.37827000	1.02999000	1.97692000
4	C	1.53405000	0.45398000	2.57233000
5	C	-2.73490000	1.2980000	0.22795000
6	C	-3.71323000	1.89475000	-0.56694000
7	C	-3.57308000	3.20152000	-1.02162000
8	C	-2.43909000	3.93646000	-0.69441000
9	C	-1.45364000	3.36616000	0.09598000
10	C	2.48675000	-0.19848000	1.75098000
11	C	3.62099000	-0.74102000	2.35358000
12	C	3.8188000	-0.65061000	3.72764000
13	C	2.88177000	-0.00814000	4.52844000
14	C	1.74720000	0.54423000	3.95230000
15	P	-2.84232000	-0.42489000	0.88328000
16	P	2.07566000	-0.38933000	-0.03629000
17	H	-4.59392000	1.33144000	-0.84101000
18	H	-4.34663000	3.63962000	-1.63875000
19	H	-2.32088000	4.94965000	-1.05480000
20	H	-0.55930000	3.91948000	0.34633000
21	H	4.36202000	-1.23936000	1.74455000
22	H	4.70896000	-1.07916000	4.16933000
23	H	3.03333000	0.06391000	5.59713000
24	H	1.01121000	1.04947000	4.56259000
25	C	-4.52317000	-0.92943000	0.31812000
26	C	-5.59564000	-0.57494000	1.14502000
27	C	-4.79081000	-1.65325000	-0.84598000
28	C	-6.89973000	-0.91089000	0.80621000
29	H	-5.40531000	-0.03001000	2.0619000
30	C	-6.09577000	-2.00410000	-1.1779000
31	H	-3.98034000	-1.94689000	-1.49809000
32	C	-7.15364000	-1.63002000	-0.35784000
33	H	-7.71604000	-0.62118000	1.45507000
34	H	-6.28414000	-2.56845000	-2.08219000
35	H	-8.16789000	-1.90205000	-0.61898000
36	C	-1.74467000	-1.32577000	-0.29085000
37	C	-1.20210000	-2.53747000	0.142980000
38	C	-1.44164000	-0.88018000	-1.57965000
39	C	-0.39528000	-3.29645000	-0.69626000
40	H	-1.40904000	-2.88511000	1.14747000
41	C	-0.62742000	-1.63414000	-2.41585000
42	H	-1.84060000	0.06196000	-1.93081000
43	C	-0.10541000	-2.84625000	-1.97848000
44	H	0.01555000	-4.23365000	-0.34345000
45	H	-0.39824000	-1.27405000	-3.41076000
46	H	0.53553000	-3.42756000	-2.62795000
47	C	3.59884000	-1.1856000	-0.69691000
48	C	3.60758000	-2.58477000	-0.72318000
49	C	4.71441000	-0.50208000	-1.18641000
50	C	4.70953000	-3.28277000	-1.20177000
51	H	2.73965000	-3.12673000	-0.36825000
52	C	5.81178000	-1.19960000	-1.67993000
53	H	4.72745000	0.57898000	-1.18677000
54	C	5.81532000	-2.59023000	-1.68431000
55	H	4.70111000	-4.36508000	-1.20791000
56	H	6.66669000	-0.65459000	-2.05915000
57	H	6.67106000	-3.13072000	-2.06712000
58	C	2.21683000	1.34264000	-0.64846000
59	C	1.48088000	1.67152000	-1.78948000
60	C	2.96719000	2.34213000	-0.02416000
61	C	1.50338000	2.96243000	-2.30370000
62	H	0.87089000	0.91340000	-2.26285000
63	C	2.98392000	3.63580000	-0.53183000
64	H	3.52967000	2.11228000	0.87101000
65	C	2.25401000	3.94902000	-1.67441000
66	H	0.92106000	3.2012000	-3.18403000
67	H	3.56605000	4.40053000	-0.03375000
68	H	2.26496000	4.95758000	-2.06663000

Table S2. Optimized coordinates for **7b** (charge = 0, multiplicity = 1).

Label	Symbol	X	Y	Z
1	C	1.634372000	-1.198000000	-1.455961000
2	C	0.493215000	-0.347864000	-1.484896000
3	C	-0.493447000	0.348724000	-1.484883000
4	C	-1.634835000	1.198545000	-1.455766000
5	C	2.823216000	-0.796453000	-0.798547000
6	C	3.899706000	-1.684343000	-0.798921000
7	C	3.821089000	-2.925749000	-1.420519000
8	C	2.646949000	-3.315075000	-2.054321000
9	C	1.558956000	-2.457123000	-2.067653000
10	C	-2.823529000	0.796592000	-0.798330000
11	C	-3.900223000	1.684234000	-0.798422000
12	C	-3.821954000	2.925776000	-1.419796000
13	C	-2.647960000	3.315498000	-2.053623000
14	C	-1.559764000	2.457807000	-2.067211000
15	P	2.810674000	0.864263000	0.015037000
16	P	-2.810490000	-0.864246000	0.014988000
17	C	-1.895759000	-0.353193000	1.589424000
18	C	-1.282165000	-1.558051000	2.309444000
19	C	-2.667248000	0.561977000	2.539778000
20	C	-4.594993000	-1.096244000	0.535576000
21	C	-4.715957000	-2.265567000	1.520979000
22	C	-5.451517000	-1.372594000	-0.708302000
23	C	1.896223000	0.353105000	1.589602000
24	C	1.282895000	1.557923000	2.309913000
25	C	2.667832000	-0.562253000	2.539677000
26	C	4.595331000	1.095827000	0.535286000
27	C	4.716728000	2.265061000	1.520741000
28	C	5.451682000	1.372083000	-0.708728000
29	H	4.820070000	-1.417316000	-0.300397000
30	H	4.675408000	-3.589859000	-1.401202000
31	H	2.578664000	-4.281604000	-2.535336000
32	H	0.636260000	-2.745488000	-2.551941000
33	H	-4.820475000	1.416903000	-0.299854000
34	H	-4.676427000	3.589682000	-1.400278000
35	H	-2.579939000	4.282141000	-2.534446000
36	H	-0.637166000	2.746496000	-2.551490000
37	H	-1.070022000	0.226466000	1.173944000
38	H	-0.690265000	-2.167887000	1.626328000
39	H	-0.624962000	-1.219793000	3.114459000
40	H	-2.041252000	-2.200391000	2.756291000
41	H	-3.064018000	1.435545000	2.021963000
42	H	-2.008095000	0.919836000	3.334895000
43	H	-3.499395000	0.043928000	3.017842000
44	H	-4.962435000	-0.195032000	1.031835000
45	H	-4.230253000	-2.059019000	2.472847000
46	H	-5.768796000	-2.471405000	1.727215000
47	H	-4.275705000	-3.176547000	1.109715000
48	H	-5.392881000	-0.572521000	-1.445527000
49	H	-6.500296000	-1.491729000	-0.425773000
50	H	-5.131529000	-2.295031000	-1.196832000
51	H	1.070340000	-0.226418000	1.174226000
52	H	0.690940000	2.167938000	1.627003000
53	H	0.625799000	1.219610000	3.114993000
54	H	2.042136000	2.200101000	2.756730000
55	H	3.064428000	-1.435785000	2.021667000
56	H	2.008810000	-0.920160000	3.334882000
57	H	3.500119000	-0.044332000	3.017639000
58	H	4.962667000	0.194501000	1.031422000
59	H	4.231129000	2.058565000	2.472672000
60	H	5.769648000	2.470642000	1.726821000
61	H	4.276622000	3.176168000	1.109602000
62	H	5.392774000	0.572062000	-1.445988000
63	H	6.500531000	1.491012000	-0.426373000
64	H	5.131782000	2.294604000	-1.197159000

Table S3. Optimized coordinates for **4a** (charge = 0, multiplicity = 1).

Label	Symbol	X	Y	Z
1	C	-0.8550140	-0.1503770	3.0332110
2	C	-0.2158760	-0.1366800	4.2569100
3	C	1.1870800	-0.1106700	4.3554750
4	C	1.9507270	-0.0893560	3.2004460
5	C	1.3231680	-0.0905210	1.9551560
6	C	-0.1083180	-0.1386530	1.8368390
7	P	2.0487550	-0.0506740	0.3297350
8	C	0.5471020	-0.1692580	-0.4935330
9	C	-0.5471120	-0.1692580	0.4935360
10	C	0.1083090	-0.1386520	-1.8368350
11	C	-1.3231770	-0.0905180	-1.9551510
12	P	-2.0487650	-0.0506720	-0.3297300
13	C	0.8550040	-0.1503770	-3.0332070
14	C	0.2158650	-0.1366770	-4.2569060
15	C	-1.1870910	-0.1106630	-4.3554700
16	C	-1.9507380	-0.0893480	-3.2004400
17	H	-1.9365730	-0.1756390	2.9880410
18	H	-0.8090450	-0.1492930	5.1627840
19	H	1.6638410	-0.1030240	5.3257320
20	H	3.0318980	-0.0641790	3.2672690
21	H	1.9365620	-0.1756410	-2.9880390
22	H	0.8090330	-0.1492910	-5.1627800
23	H	-1.6638530	-0.1030160	-5.3257260
24	H	-3.0319080	-0.0641680	-3.2672630
25	C	-3.2086620	-1.4110770	0.0383560
26	C	-4.5142360	-1.4090340	-0.4602000
27	C	-2.7489960	-2.5127230	0.7605360
28	C	-5.3465480	-2.4986140	-0.2408040
29	H	-4.8836630	-0.5527190	-1.0094870
30	C	-3.5907240	-3.5933720	0.9950000
31	H	-1.7332460	-2.5106070	1.1346500
32	C	-4.8870640	-3.5902040	0.4907020
33	H	-6.3546730	-2.4944600	-0.6340260
34	H	-3.2332910	-4.4384540	1.5684480
35	H	-5.5390620	-4.4357040	0.6667420
36	C	-3.0695740	1.4501540	-0.1002370
37	C	-2.8634610	2.5569150	-0.9284050
38	C	-3.9385470	1.5654110	0.9897970
39	C	-3.5302610	3.7498650	-0.6815880
40	H	-2.1811270	2.4780910	-1.7642130
41	C	-4.5929730	2.7639660	1.2418460
42	H	-4.1098820	0.7159550	1.6381970
43	C	-4.3932140	3.8574650	0.4048680
44	H	-3.3741210	4.5971760	-1.3363160
45	H	-5.2613060	2.8439090	2.0892170
46	H	-4.9068460	4.7896840	0.5995470
47	C	3.2086550	-1.4110750	-0.0383550
48	C	4.5142370	-1.4090100	0.4601790
49	C	2.7489910	-2.5127280	-0.7605240
50	C	5.3465580	-2.4985840	0.2407810
51	H	4.8836640	-0.5526850	1.0094500
52	C	3.5907260	-3.5933710	-0.9949910
53	H	1.7332360	-2.5106250	-1.1346240
54	C	4.8870730	-3.5901850	-0.4907090
55	H	6.3546880	-2.4944160	0.6339870
56	H	3.2332950	-4.4384600	-1.5684270
57	H	5.5390770	-4.4356800	-0.6667510
58	C	3.0695710	1.4501450	0.1002410
59	C	2.8634490	2.5569220	0.9283860
60	C	3.9385740	1.5653740	-0.9897720
61	C	3.5302600	3.7498640	0.6815610
62	H	2.1810930	2.4781190	1.7641790
63	C	4.5930130	2.7639200	-1.2418290
64	H	4.1099230	0.7159020	-1.6381480
65	C	4.3932380	3.8574380	-0.4048780
66	H	3.3741090	4.5971890	1.3362680
67	H	5.2613690	2.8438420	-2.0891830
68	H	4.9068800	4.7896500	-0.5995630

Table S4. Optimized coordinates for **4b** (charge = 0, multiplicity = 1).

Label	Symbol	X	Y	Z
1	C	0.2581520	-3.1364330	0.0866150
2	C	-0.6197250	-4.1965070	0.1616620
3	C	-2.0125220	-4.0000030	0.1773190
4	C	-2.5109370	-2.7108970	0.1060180
5	C	-1.6415700	-1.6205830	0.0196080
6	C	-0.2117420	-1.8035280	0.0190760
7	P	-2.0181490	0.1200620	-0.0384890
8	C	-0.3692220	0.6237800	-0.0466110
9	C	0.5009380	-0.5866780	-0.0339400
10	C	0.3494620	1.8394290	-0.0965930
11	C	1.7779490	1.6461050	-0.1027030
12	P	2.1482740	-0.0925190	-0.0600670
13	C	-0.0999190	3.1808200	-0.1357970
14	C	0.7936190	4.2313370	-0.1668390
15	C	2.1839710	4.0209910	-0.1603170
16	C	2.6639860	2.7226310	-0.1266440
17	C	3.1416890	-0.5875140	-1.5637990
18	C	2.8874170	-2.0295910	-2.0119160
19	C	4.6354880	-0.2625650	-1.4659130
20	C	3.1980920	-0.4785520	1.4293970
21	C	2.5000300	0.0625670	2.6806060
22	C	3.5272090	-1.9666170	1.5864140
23	C	-2.9856980	0.5690910	-1.5800540
24	C	-3.4771380	2.0199810	-1.6119240
25	C	-4.1028760	-0.4142850	-1.9478070
26	C	-2.9981440	0.6094030	1.4760240
27	C	-4.4794280	0.2212240	1.4545800
28	C	-2.7925530	2.0730570	1.8773610
29	H	1.3217710	-3.3291620	0.0798120
30	H	-0.2259750	-5.2041800	0.2128520
31	H	-2.6840700	-4.8445380	0.2426300
32	H	-3.5823140	-2.5576040	0.1146160
33	H	-1.1593820	3.3932040	-0.1275870
34	H	0.4118470	5.2446280	-0.1924600
35	H	2.8655310	4.8597420	-0.1789480
36	H	3.7335310	2.5495370	-0.1109570
37	H	2.6957010	0.0726640	-2.3128690
38	H	1.8216310	-2.2389630	-2.0874940
39	H	3.3362500	-2.1915200	-2.9943090
40	H	3.3292860	-2.7557510	-1.3293560
41	H	4.8139040	0.7769900	-1.1908600
42	H	5.1133320	-0.4308880	-2.4333450
43	H	5.1407710	-0.8980750	-0.7381090
44	H	4.1265200	0.0792520	1.2702630
45	H	2.2953120	1.1292440	2.6004020
46	H	1.5504640	-0.4510530	2.8391930
47	H	3.1288800	-0.1031630	3.5576890
48	H	2.6202890	-2.5484180	1.7517370
49	H	4.1717900	-2.1115970	2.4557000
50	H	4.0445680	-2.3797710	0.7221750
51	H	-2.1945410	0.4650220	-2.3273590
52	H	-2.6768420	2.7299430	-1.4126430
53	H	-3.8762620	2.2472170	-2.6027990
54	H	-4.2779130	2.1923690	-0.8931200
55	H	-3.7381110	-1.4383780	-1.9948820
56	H	-4.4974810	-0.1559580	-2.9331750
57	H	-4.9346340	-0.3766720	-1.2458500
58	H	-2.4958690	-0.0101180	2.2243220
59	H	-4.6289810	-0.8274050	1.2004480
60	H	-4.9119100	0.3827070	2.4443160
61	H	-5.0475070	0.8281700	0.7503890
62	H	-1.7347170	2.3216850	1.9394800
63	H	-3.2391730	2.2473180	2.8587500
64	H	-3.2667270	2.7603970	1.1767510

Table S5. Optimized coordinates for **5a** (charge = 1, multiplicity = 2).

Label	Symbol	X	Y	Z
1	C	3.6500430	3.7648520	0.1915050
2	C	4.5310240	3.5745490	1.2511460
3	C	-3.2625070	3.8133740	-0.0837630
4	C	-4.5770720	3.7819540	0.3686290
5	C	2.9281500	2.6929800	-0.3159570
6	C	4.6978680	2.3079650	1.8025900
7	C	-2.5085760	2.6473400	-0.1142380
8	C	-5.1460450	2.5819810	0.7861740
9	C	3.0970320	1.4182770	0.2324280
10	C	3.9870330	1.2294770	1.2950570
11	C	1.1592590	0.8649130	-4.2825870
12	C	-0.2338590	0.8619320	-4.1710780
13	C	-3.0791680	1.4411620	0.2983460
14	C	1.9450290	0.6271020	-3.1606620
15	C	-4.4034200	1.4105660	0.7480850
16	C	-0.8602880	0.6241800	-2.9560480
17	C	1.3268170	0.3926710	-1.9398820
18	C	-0.0908030	0.3829730	-1.8133360
19	C	-0.5202440	0.1188150	-0.4688080
20	C	0.5202440	-0.1188150	0.4688080
21	C	0.0908030	-0.3829730	1.8133360
22	C	-1.3268170	-0.3926710	1.9398820
23	C	4.4034200	-1.4105660	-0.7480850
24	C	0.8602880	-0.6241800	2.9560480
25	C	-1.9450290	-0.6271020	3.1606620
26	C	3.0791680	-1.4411620	-0.2983460
27	C	0.2338590	-0.8619320	4.1710780
28	C	-1.1592590	-0.8649130	4.2825870
29	C	-3.9870330	-1.2294770	-1.2950570
30	C	-3.0970320	-1.4182770	-0.2324280
31	C	5.1460450	-2.5819810	-0.7861740
32	C	2.5085760	-2.6473400	0.1142380
33	C	-4.6978680	-2.3079650	-1.8025900
34	C	-2.9281500	-2.6929800	0.3159570
35	C	4.5770720	-3.7819540	-0.3686290
36	C	3.2625070	-3.8133740	0.0837630
37	C	-4.5310240	-3.5745490	-1.2511460
38	C	-3.6500430	-3.7648520	-0.1915050
39	H	3.5262940	4.7479930	-0.2415020
40	H	5.0905540	4.4120510	1.6449750
41	H	-2.8236080	4.7454460	-0.4122370
42	H	-5.1606900	4.6921320	0.3942990
43	H	2.2429590	2.8439630	-1.1388360
44	H	5.3854070	2.1591770	2.6238510
45	H	-1.4839370	2.6701290	-0.4596600
46	H	-6.1689710	2.5585930	1.1359410
47	H	1.6255730	1.0498810	-5.2396810
48	H	-0.8364140	1.0458940	-5.0504070
49	H	3.0241130	0.6266240	-3.2445230
50	H	4.1345760	0.2443200	1.7166420
51	H	-1.9402100	0.6221720	-2.8941900
52	H	-4.8559750	0.4777460	1.0571920
53	H	4.8559750	-0.4777460	-1.0571920
54	H	-4.1345760	-0.2443200	-1.7166420
55	H	1.9402100	-0.6221720	2.8941900
56	H	-3.0241130	-0.6266240	3.2445230
57	H	0.8364140	-1.0458940	5.0504070
58	H	-1.6255730	-1.0498810	5.2396810
59	H	6.1689710	-2.5585930	-1.1359410
60	H	-5.3854070	-2.1591770	-2.6238510
61	H	1.4839370	-2.6701290	0.4596600
62	H	-2.2429590	-2.8439630	1.1388360
63	H	5.1606900	-4.6921320	-0.3942990
64	H	2.8236080	-4.7454460	0.4122370
65	H	-5.0905540	-4.4120510	-1.6449750
66	H	-3.5262940	-4.7479930	0.2415020
67	P	2.0672790	0.0512370	-0.3433640
68	P	-2.0672790	-0.0512370	0.3433640

Table S6. Optimized coordinates for **5b** (charge = 1, multiplicity = 2).

Label	Symbol	X	Y	Z
1	C	0.1791020	-3.1188970	0.0959900
2	C	-0.7128960	-4.1921990	0.1552900
3	C	-2.0873960	-3.9780010	0.1432900
4	C	-2.5997980	-2.6780020	0.0678900
5	C	-1.7167000	-1.6100000	0.0046900
6	C	-0.3128000	-1.8186980	0.0227900
7	P	-2.0716030	0.1659990	-0.0511100
8	C	-0.2932030	0.5997020	-0.0543100
9	C	0.4328990	-0.5609970	-0.0256100
10	C	0.4616950	1.8566030	-0.0915100
11	C	1.8638950	1.6346050	-0.0805100
12	P	2.2073980	-0.1401940	-0.0536100
13	C	-0.0094070	3.1663020	-0.1155100
14	C	0.8981910	4.2287040	-0.1263100
15	C	2.2696920	3.9982060	-0.1047100
16	C	2.7631940	2.6887060	-0.0787100
17	C	3.0483990	-0.6494930	-1.6193100
18	C	2.8201010	-2.1153930	-2.0035100
19	C	4.5364980	-0.2743910	-1.5489100
20	C	3.0879990	-0.5757930	1.5058900
21	C	2.2717980	-0.0794940	2.7071900
22	C	3.4571010	-2.0583930	1.6209900
23	C	-2.8813030	0.6504980	-1.6471100
24	C	-3.3220050	2.1188970	-1.6713100
25	C	-4.0285020	-0.3047040	-2.0099100
26	C	-2.9090030	0.6741980	1.5194900
27	C	-4.3925030	0.2768960	1.5009900
28	C	-2.7006050	2.1473980	1.8861900
29	H	1.2437030	-3.3104960	0.1033900
30	H	-0.3272940	-5.2030980	0.2120900
31	H	-2.7679950	-4.8193020	0.1910900
32	H	-3.6716980	-2.5278030	0.0561900
33	H	-1.0695070	3.3774010	-0.1145100
34	H	0.5251900	5.2458030	-0.1451100
35	H	2.9606900	4.8323070	-0.1051100
36	H	3.8331940	2.5199080	-0.0504100
37	H	2.5564980	-0.0111940	-2.3616100
38	H	1.7632010	-2.3551950	-2.1201100
39	H	3.3020010	-2.2961930	-2.9662100
40	H	3.2639020	-2.8091930	-1.2888100
41	H	4.6975970	0.7837090	-1.3364100
42	H	4.9924980	-0.4754900	-2.5198100
43	H	5.0753990	-0.8669900	-0.8080100
44	H	4.0081980	0.0163080	1.4292900
45	H	2.0397960	0.9845050	2.6447900
46	H	1.3393990	-0.6385960	2.8115900
47	H	2.8524980	-0.2371930	3.6173900
48	H	2.5721020	-2.6863940	1.7311900
49	H	4.0599010	-2.1961920	2.5203900
50	H	4.0479010	-2.4199920	0.7798900
51	H	-2.0700030	0.5073990	-2.3700100
52	H	-2.5025070	2.8127980	-1.4881100
53	H	-3.7122060	2.3443970	-2.6652100
54	H	-4.1225060	2.3183960	-0.9585100
55	H	-3.6978000	-1.3392030	-2.0939100
56	H	-4.4195020	-0.0099040	-2.9854100
57	H	-4.8557020	-0.2508050	-1.3018100
58	H	-2.3875020	0.0519990	2.2555900
59	H	-4.5502010	-0.7773050	1.2702900
60	H	-4.8074030	0.4504950	2.4952900
61	H	-4.9684040	0.8808950	0.7992900
62	H	-1.6472060	2.4031000	1.9981900
63	H	-3.1821060	2.3311970	2.8485900
64	H	-3.1577070	2.8252970	1.1647900

Table S7. Optimized coordinates for **6a** (charge = 2, multiplicity = 1).

Label	Symbol	X	Y	Z
1	C	-3.5612310	3.8007910	-0.0001580
2	C	-4.4290120	3.6713990	-1.0802170
3	C	3.1009170	3.8566020	0.0754440
4	C	4.4570710	3.8516650	-0.2389060
5	C	-2.8631000	2.6969270	0.4684440
6	C	-4.6074610	2.4355020	-1.6968400
7	C	2.3791990	2.6725130	0.0596560
8	C	5.0999690	2.6619300	-0.5686400
9	C	-3.0431500	1.4536180	-0.1502780
10	C	-3.9186830	1.3236640	-1.2369720
11	C	-1.0779660	0.6805510	4.3440710
12	C	0.3047660	0.6815140	4.2032870
13	C	3.0268810	1.4746830	-0.2665910
14	C	-1.9026600	0.4937080	3.2312950
15	C	4.3916110	1.4692370	-0.5837740
16	C	0.8998260	0.4947060	2.9549080
17	C	-1.3136950	0.3121300	1.9939460
18	C	0.0918400	0.3062060	1.8426360
19	C	0.4945060	0.0893890	0.4564740
20	C	-0.4945060	-0.0893890	-0.4564740
21	C	-0.0918400	-0.3062060	-1.8426360
22	C	1.3136950	-0.3121300	-1.9939460
23	C	-4.3916110	-1.4692370	0.5837740
24	C	-0.8998260	-0.4947060	-2.9549080
25	C	1.9026600	-0.4937080	-3.2312950
26	C	-3.0268810	-1.4746830	0.2665910
27	C	-0.3047660	-0.6815140	-4.2032870
28	C	1.0779660	-0.6805510	-4.3440710
29	C	3.9186830	-1.3236640	1.2369720
30	C	3.0431500	-1.4536180	0.1502780
31	C	-5.0999690	-2.6619300	0.5686400
32	C	-2.3791990	-2.6725130	-0.0596560
33	C	4.6074610	-2.4355020	1.6968400
34	C	2.8631000	-2.6969270	-0.4684440
35	C	-4.4570710	-3.8516650	0.2389060
36	C	-3.1009170	-3.8566020	-0.0754440
37	C	4.4290120	-3.6713990	1.0802170
38	C	3.5612310	-3.8007910	0.0001580
39	H	-3.4342760	4.7598610	0.4822180
40	H	-4.9738880	4.5339540	-1.4385920
41	H	2.6079140	4.7831450	0.3342910
42	H	5.0153780	4.7776020	-0.2244840
43	H	-2.1976240	2.8007500	1.3141120
44	H	-5.2891330	2.3376010	-2.5301120
45	H	1.3253260	2.6834420	0.3025410
46	H	6.1534820	2.6622880	-0.8108210
47	H	-1.5209920	0.8237550	5.3194450
48	H	0.9294510	0.8272770	5.0735550
49	H	-2.9781420	0.4923640	3.3477260
50	H	-4.0767210	0.3625780	-1.7068080
51	H	1.9766280	0.4966680	2.8614900
52	H	4.8987900	0.5465070	-0.8308480
53	H	-4.8987900	-0.5465070	0.8308480
54	H	4.0767210	-0.3625780	1.7068080
55	H	-1.9766280	-0.4966680	-2.8614900
56	H	2.9781420	-0.4923640	-3.3477260
57	H	-0.9294510	-0.8272770	-5.0735550
58	H	1.5209920	-0.8237550	-5.3194450
59	H	-6.1534820	-2.6622880	0.8108210
60	H	5.2891330	-2.3376010	2.5301120
61	H	-1.3253260	-2.6834420	-0.3025410
62	H	2.1976240	-2.8007500	-1.3141120
63	H	-5.0153780	-4.7776020	0.2244840
64	H	-2.6079140	-4.7831450	-0.3342910
65	H	4.9738880	-4.5339540	1.4385920
66	H	3.4342760	-4.7598610	-0.4822180
67	P	-2.0935480	0.0408420	0.3911280
68	P	2.0935480	-0.0408420	-0.3911280

Table S8. Optimized coordinates for **6b** (charge = 2, multiplicity = 1).

Label	Symbol	X	Y	Z
1	C	0.1757790	-3.1078760	0.1305570
2	C	-0.7107310	-4.1817480	0.1876030
3	C	-2.0836930	-3.9720930	0.1619760
4	C	-2.5980640	-2.6768440	0.0773190
5	C	-1.7199550	-1.6065650	0.0209000
6	C	-0.3202080	-1.8123660	0.0486040
7	P	-2.0657480	0.1607470	-0.0407090
8	C	-0.2964420	0.5997980	-0.0266150
9	C	0.4256790	-0.5579530	0.0014700
10	C	0.4613100	1.8529420	-0.0625280
11	C	1.8592510	1.6302140	-0.0579160
12	P	2.1909600	-0.1360680	-0.0490590
13	C	-0.0096570	3.1602360	-0.0794980
14	C	0.8956850	4.2207560	-0.0891530
15	C	2.2651470	3.9904390	-0.0724340
16	C	2.7567910	2.6836190	-0.0533750
17	C	2.9848070	-0.6322980	-1.6350510
18	C	2.7598070	-2.0956190	-2.0325220
19	C	4.4723060	-0.2459490	-1.6245800
20	C	3.1197790	-0.5890180	1.4684800
21	C	2.3467200	-0.1352490	2.7149830
22	C	3.5348580	-2.0619100	1.5516340
23	C	-2.8471780	0.6434840	-1.6432540
24	C	-3.2650770	2.1183620	-1.6967660
25	C	-4.0059590	-0.2898040	-2.0295840
26	C	-2.9294170	0.6721450	1.5057470
27	C	-4.4142360	0.2777490	1.4685150
28	C	-2.7327010	2.1435440	1.8866350
29	H	1.2390020	-3.2923010	0.1451600
30	H	-0.3237060	-5.1891990	0.2515910
31	H	-2.7604890	-4.8136060	0.2062650
32	H	-3.6679900	-2.5311550	0.0532150
33	H	-1.0675980	3.3681510	-0.0700250
34	H	0.5237890	5.2358400	-0.1018750
35	H	2.9546570	4.8226950	-0.0706420
36	H	3.8244490	2.5156060	-0.0282130
37	H	2.4604820	0.0069500	-2.3517780
38	H	1.7041100	-2.3475480	-2.1101640
39	H	3.2077600	-2.2530990	-3.0135960
40	H	3.2382980	-2.7901820	-1.3445030
41	H	4.6352050	0.8078380	-1.4027170
42	H	4.8822100	-0.4321720	-2.6167870
43	H	5.0423810	-0.8465700	-0.9168890
44	H	4.0206370	0.0261020	1.3645460
45	H	2.0730070	0.9181930	2.6785660
46	H	1.4443280	-0.7310100	2.8546480
47	H	2.9785720	-0.2836870	3.5899670
48	H	2.6730030	-2.7121410	1.6945430
49	H	4.1783510	-2.1866270	2.4222630
50	H	4.0952050	-2.3989630	0.6827480
51	H	-2.0258390	0.4798490	-2.3480530
52	H	-2.4440040	2.8022590	-1.4965840
53	H	-3.6240850	2.3341410	-2.7027250
54	H	-4.0809340	2.3314560	-1.0085090
55	H	-3.7014390	-1.3323120	-2.0839470
56	H	-4.3531980	0.0009270	-3.0208210
57	H	-4.8513940	-0.2000840	-1.3500990
58	H	-2.4200020	0.0491580	2.2474630
59	H	-4.5740990	-0.7682520	1.2129790
60	H	-4.8330580	0.4343520	2.4621560
61	H	-4.9777040	0.8988330	0.7742660
62	H	-1.6838580	2.4023720	2.0139280
63	H	-3.2298150	2.3155400	2.8412950
64	H	-3.1820100	2.8204850	1.1619770

To allow for an accurate comparison to the CV data (recorded in CH_2Cl_2 , see article), the polarizable continuum model (PCM) was employed to correct for solvent effects using with the standard parameters for CH_2Cl_2 (B3LYP-D3/def2TZVPP,⁶⁻⁸ single point corrected for CH_2Cl_2).¹⁰ MO energy diagrams and isodensity plots of the frontier orbitals of **4a**, **4b**, **5a**, **5b** and **6a** are provided below (the corresponding plot for **6b** is shown in the article, c.f. Figure 7).

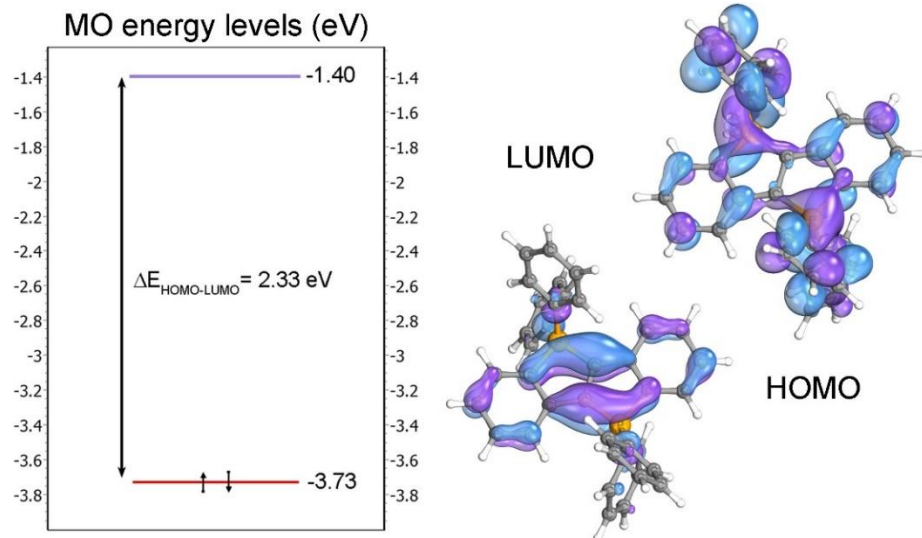


Figure S27. MO energy diagram of **4a** (B3LYP-D3/def2TZVPP, PCM solvent-corrected for CH_2Cl_2) together with isodensity plots of the Kohn-Sham HOMO and LUMO of **4a**.

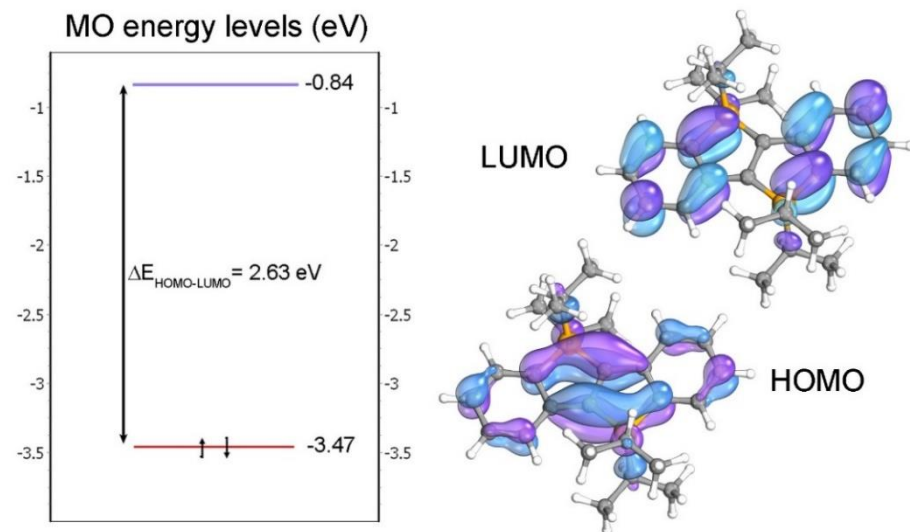


Figure S28. MO energy diagram of **4b** (B3LYP-D3/def2TZVPP, PCM solvent-corrected for CH_2Cl_2) together with isodensity plots of the Kohn-Sham HOMO and LUMO of **4b**.

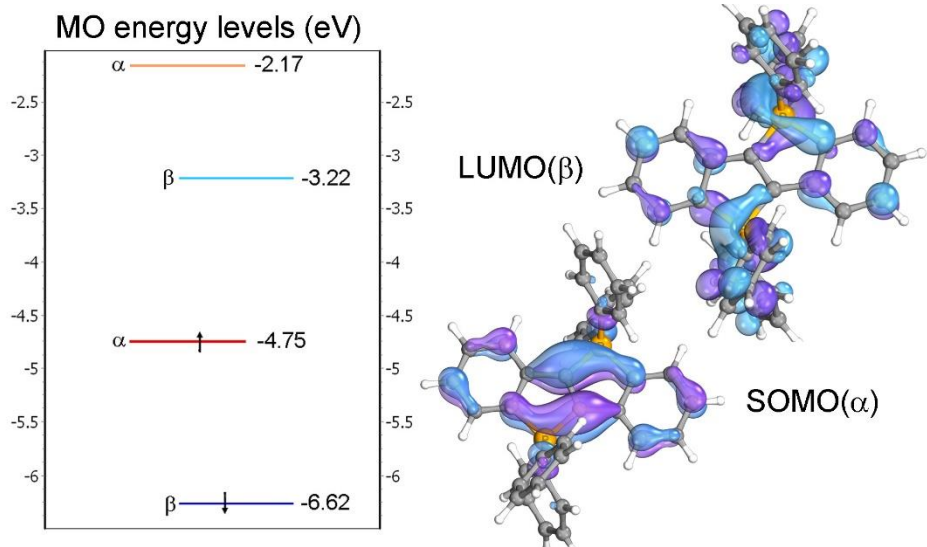


Figure S29. MO energy diagram of **5a** (UB3LYP-D3/def2TZVPP, PCM solvent-corrected for CH₂Cl₂) together with isodensity plots of the Kohn-Sham highest SOMO and LUMO of **5a**.

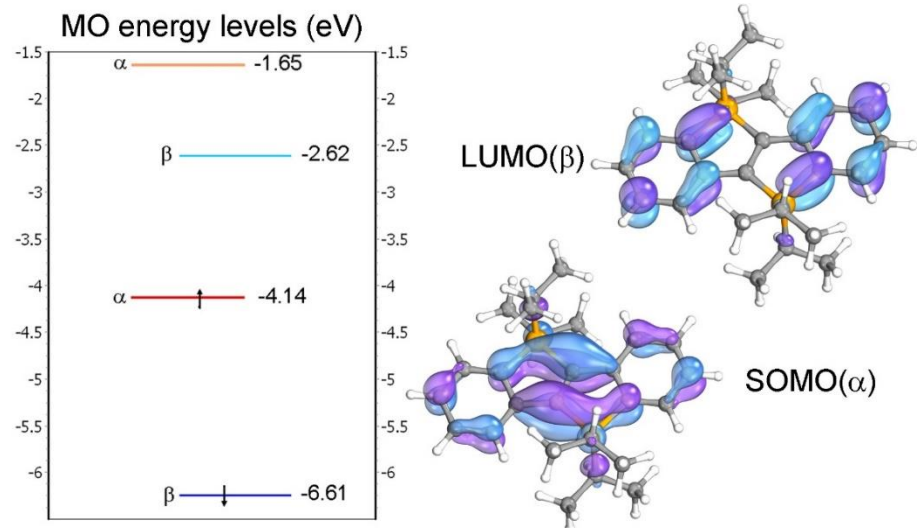


Figure S30. MO energy diagram of **5b** (UB3LYP-D3/def2TZVPP, PCM solvent-corrected for CH₂Cl₂) together with isodensity plots of the Kohn-Sham highest SOMO and LUMO of **5b**.

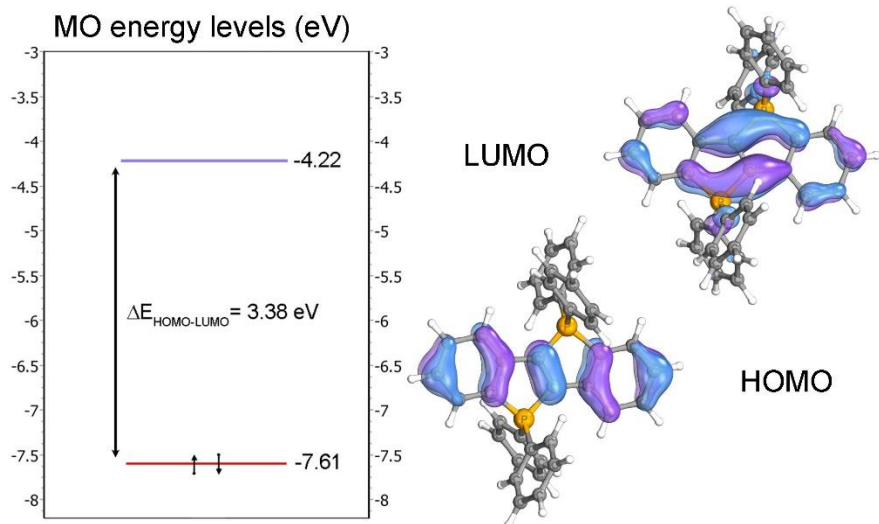


Figure S31. MO energy diagram of **6a** (B3LYP-D3/def2TZVPP, PCM solvent-corrected for CH₂Cl₂) together with isodensity plots of the Kohn-Sham HOMO and LUMO of **6a**.

The Aroma program suite¹¹ was used for the calculation of NICS(1)_{oop} values using fully optimized structures at the B3LYP/6-311G* level of theory.⁶ The out-of-plane components of the chemical shifts were used instead of the more common NICS(1)_{πZZ} values, given that the construction of σ -only models is not supported for ring systems containing doubly substituted heteroatoms.¹⁰ In our case, the addition of hydrogen atoms perpendicular to the ring system (i.e. the construction of σ -only models) interfered with the Ph- and i Pr-substituents at the phosphorus atoms. In some cases, close contacts between these substituents and the added dummy atoms were noticed as well and corrected by manually rotating the substituents and re-optimizing the molecular structure. Although reasonable results were obtained employing this methodology, a comparison to literature values is difficult. To allow for a meaningful comparison, NICS(1)_{oop} values were also calculated for a number of (hetero-substituted) pentalenes and dibenzo[a,e]pentalenes. These data are provided below.

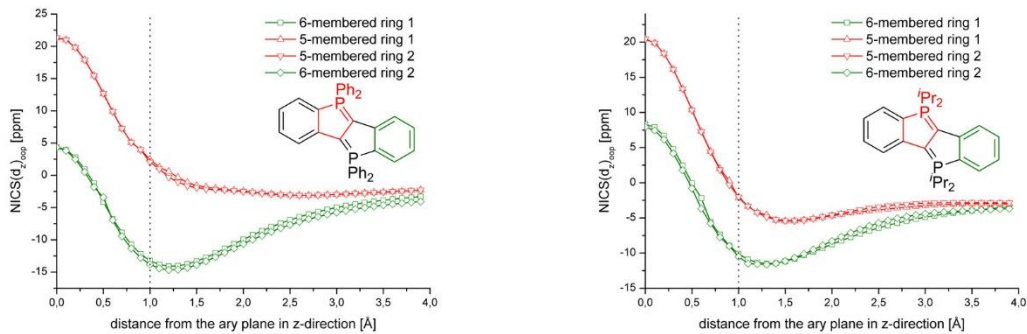


Figure S32. Plot of NICS(d_z)_{oop} values along the z axis for **4a** and **4b**.

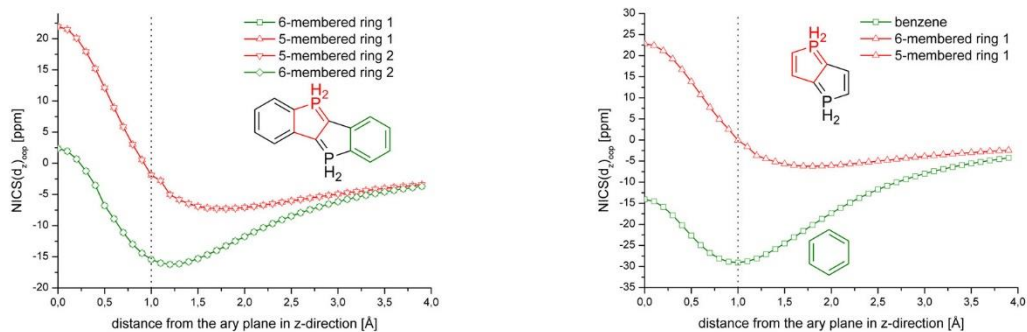


Figure S33. Plot of NICS(d_z)_{oop} values along the z axis for unsubstituted **4** together with the corresponding plots for unsubstituted diphosphapentalene and benzene.

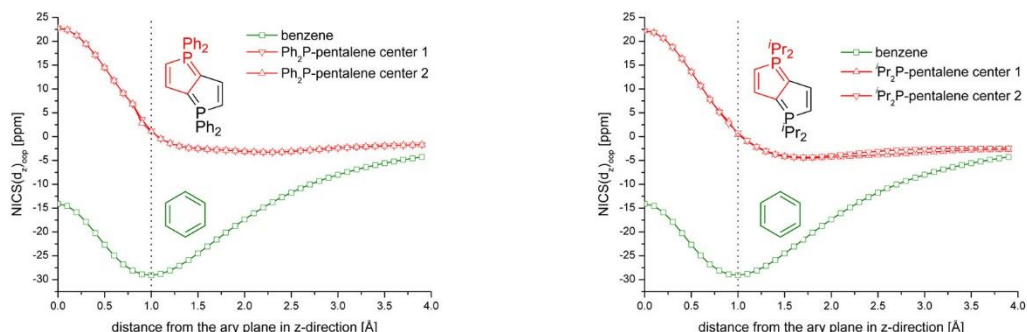


Figure S34. Plot of NICS(d_z)_{oop} values along the z axis for the Ph₂P- and i Pr₂P-substituted diphosphapentalenes together with the corresponding plot for benzene.

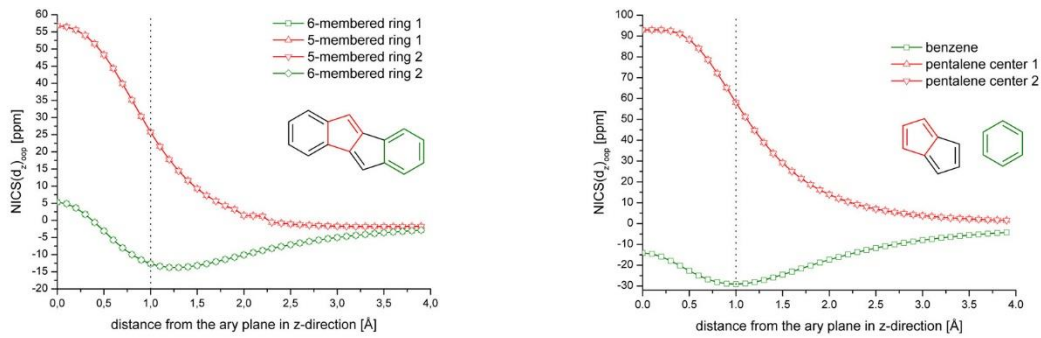


Figure S35. Plot of $\text{NICS}(d_z)_{\text{oop}}$ values along the z axis for dibenz[a,e]pentalene, parent pentalene and benzene.

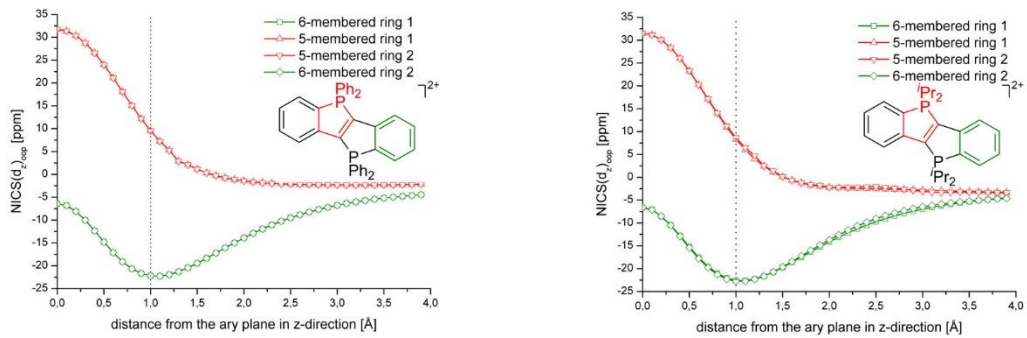


Figure S36. Plot of $\text{NICS}(d_z)_{\text{oop}}$ values along the z axis for **6a** and **6b**.

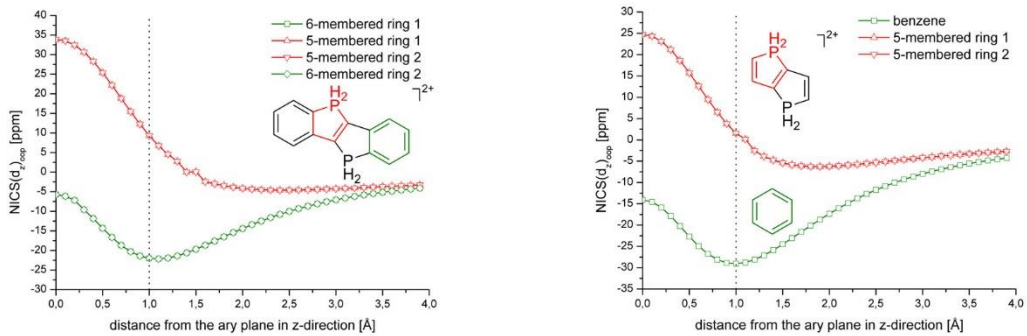


Figure S37. Plot of $\text{NICS}(d_z)_{\text{oop}}$ values along the z axis for unsubstituted **6** together with the corresponding plots for unsubstituted diphosphapentalene dication and benzene.

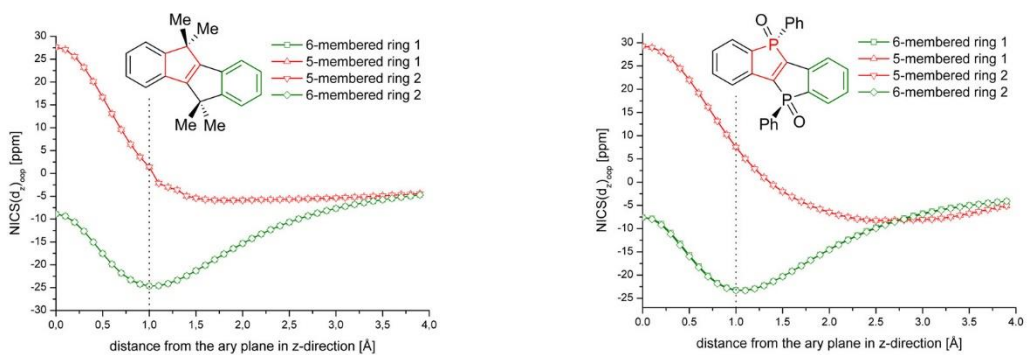


Figure S38. Plot of $\text{NICS}(d_z)_{\text{oop}}$ values along the z axis for **3c** ($R = \text{Me}$) and *trans*-**3i**.

The exchange-correlated CAM-B3YLP functional¹² was employed for TD-DFT calculations (GD3-corrected⁸ def2-TZVPP basis set^{6,7}). To allow for a comparison to UV-Vis data (recorded in MeCN for **6a**, recorded in water for **6b**), the structures were fully optimized using the polarizable continuum model (PCM) to correct for solvent effects either for MeCN (**6a**) or for water (**6b**).⁹ An oscillator strength of $f = 0.19$ (**6a**) and $f = 0.24$ (**6b**) was calculated for the lowest-energy transition at ${}^{\text{DFT}}\lambda = 385 \text{ nm}$ (**6a**, exp. $\lambda = 417 \text{ nm}$, $\Delta(\text{exp.-calcd.}) = 32 \text{ nm}$) and ${}^{\text{DFT}}\lambda = 371 \text{ nm}$ (**6b**, exp. $\lambda = 399 \text{ nm}$, $\Delta(\text{exp.-calcd.}) = 28 \text{ nm}$), respectively. The TD-DFT-modeled UV-Vis spectra are shown below.

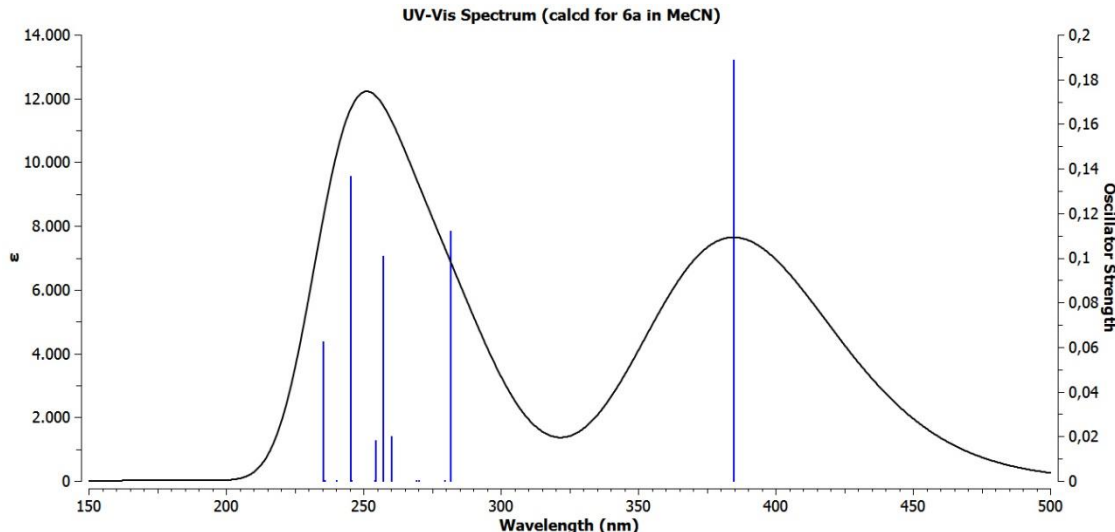


Figure S39. Calculated UV-Vis absorption spectrum of **6a** (solvent-corrected for MeCN).

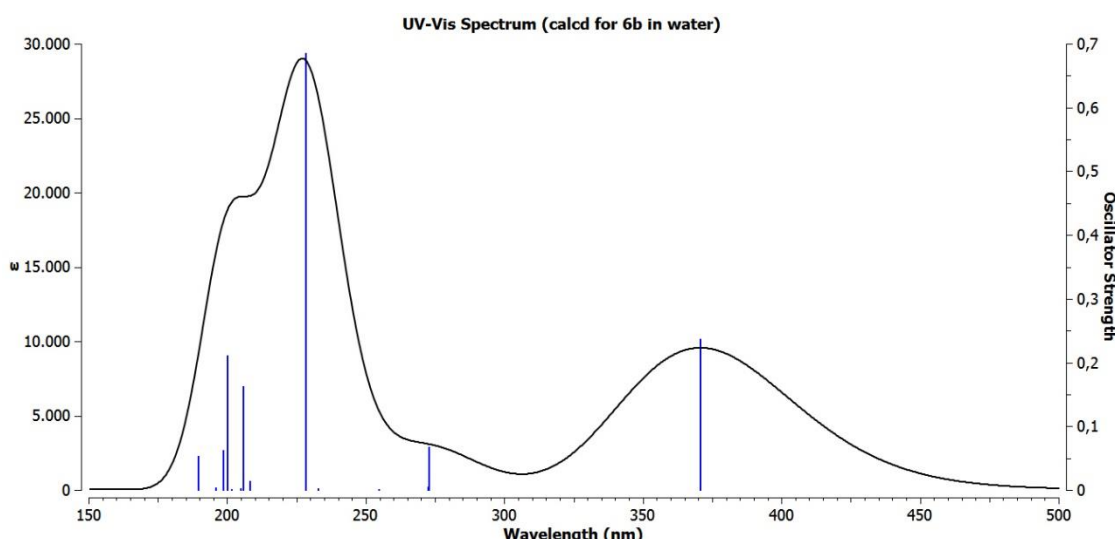


Figure S40. Calculated UV-Vis absorption spectrum of **6b** (solvent-corrected for water).

X-Ray Crystal Structure Determinations

Crystal data and details of the structure determinations are compiled in Table S9. Full shells of intensity data were collected at low temperature with an Agilent Technologies Supernova-E CCD diffractometer (Mo- K_{α} radiation, microfocus X-ray tube, multilayer mirror optics). Detector frames (typically ω , occasionally φ -scans, scan width 0.5°) were integrated by profile fitting.^{13, 14} Data were corrected for air and detector absorption, Lorentz and polarization effects¹³ and scaled essentially by application of appropriate spherical harmonic functions.^{13, 15, 16} Absorption by the crystal was treated with a semiempirical multiscan method (as part of the scaling process) and augmented by a spherical correction,^{13, 14, 15} or numerically (Gaussian grid).¹³⁻¹⁷ An illumination correction was performed as part of the numerical absorption correction.¹⁴ The structures were solved by the charge flip procedure¹⁸ and refined by full-matrix least squares methods based on F^2 against all unique reflections.¹⁹ All non-hydrogen atoms were given anisotropic displacement parameters. Hydrogen atoms were generally input at calculated positions and refined with a riding model. When justified by the quality of the data the positions of some hydrogen atoms were taken from difference Fourier syntheses and refined.

CCDC 1884989 - 1884992 contains the supplementary crystallographic data for this paper. These data can be obtained free of charge from the Cambridge Crystallographic Data Centre's and FIZ Karlsruhe's joint Access Service via <https://www.ccdc.cam.ac.uk>.

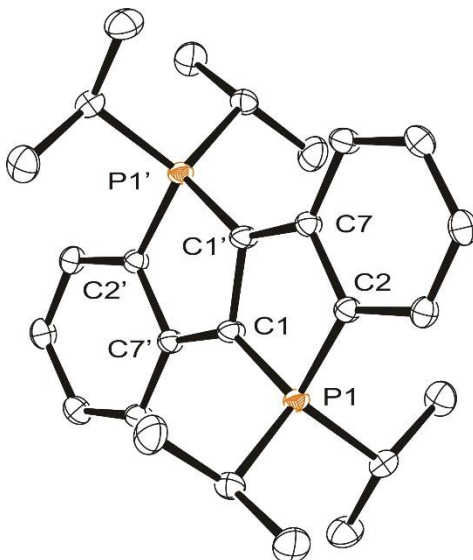


Figure S41. ORTEP plot of the molecular structure of **4b** (only one of the two independent C_s -symmetric molecules is shown; displacement ellipsoids drawn at 50% probability, hydrogen atoms omitted for clarity). Selected bond lengths (Å) and angles (°) [values in square brackets refer to the second molecule]: P1-C1 1.7210(10) [1.7210(11)], P1-C2 1.7742(10) [1.7760(11)], C1-C1' 1.486(2) [1.484(2)], C1-C7' 1.4142(14) [1.4094(14)], C2-C7 1.4431(14) [1.4407(15)], C1-P1-C2 94.94(5) [94.71(5)], C1'-C1-P1 108.83(9) [108.94(9)], C7'-C1-P1 137.31(8) [137.21(8)], C7'-C1-C1' 113.79(11) [113.79(11)], C1'-C7-C2 112.92(9) [113.05(9)].

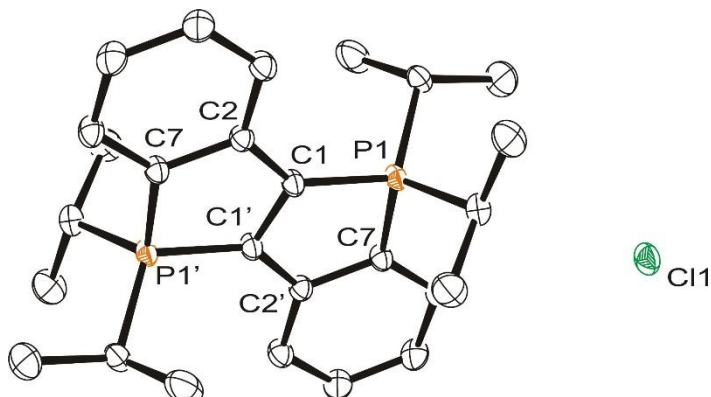


Figure S42. ORTEP plot of the molecular structure of **5b**·2C₂H₄Cl₂ (only one of the two independent C_s -symmetric molecules is shown, displacement ellipsoids drawn at 50% probability, hydrogen atoms and co-crystallized solvent molecules omitted for clarity). Selected bond lengths (Å) and angles (°) [values in square brackets refer to the second molecule]: P1-C1 1.7599(15) [1.7509(15)], P1-C7 1.7886(16) [1.7897(15)], C1-C1' 1.424(3) [1.429(3)], C1-C2 1.436(2) [1.438(2)], C2-C7' 1.419(2) [1.421(2)], C1-P1-C7 93.69(7) [93.91(7)], C1'-C1-P1 108.73(14) [108.99(14)], C1'-C1-C2 115.42(16) [114.94(16)], C2-C1-P1 135.84(12) [136.07(11)], C7'-C2-C1 112.40(13) [112.65(13)], C2'-C7-P1 109.73(11) [109.39(11)].

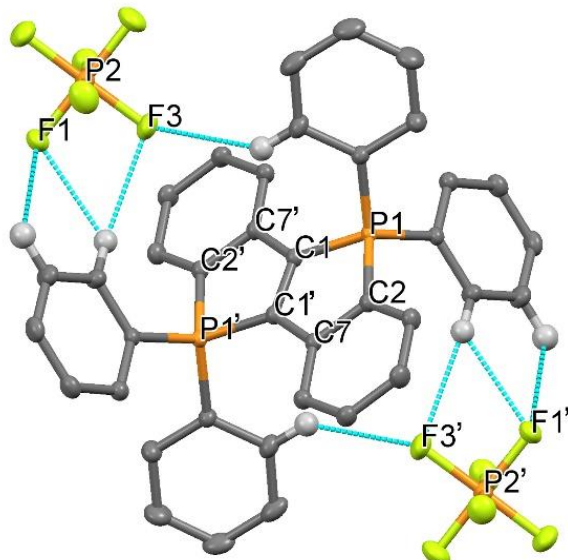


Figure S43. Mercury plot of the molecular structure of **6a** showing selected short contacts between the dicationic fragment and the $[PF_6]^-$ -counter ions (displacement ellipsoids drawn at 50% probability, hydrogen atoms – expect those exhibiting short contacts to fluorine atoms – omitted for clarity). Selected bond lengths (\AA) and angles ($^\circ$): P1–C1 1.7990(12), P1–C2 1.7916(13), C1–C1' 1.359(2), C1–C7' 1.4648(17), C2–C7 1.4139(17), C2–P1–C1 93.05(6), C1'–C1–P1 108.67(12), C1'–C1–C7' 116.89(14), C7'–C1–P1 134.42(10), C7–C2–P1 109.58(9), C2–C7–C1' 111.76(11).

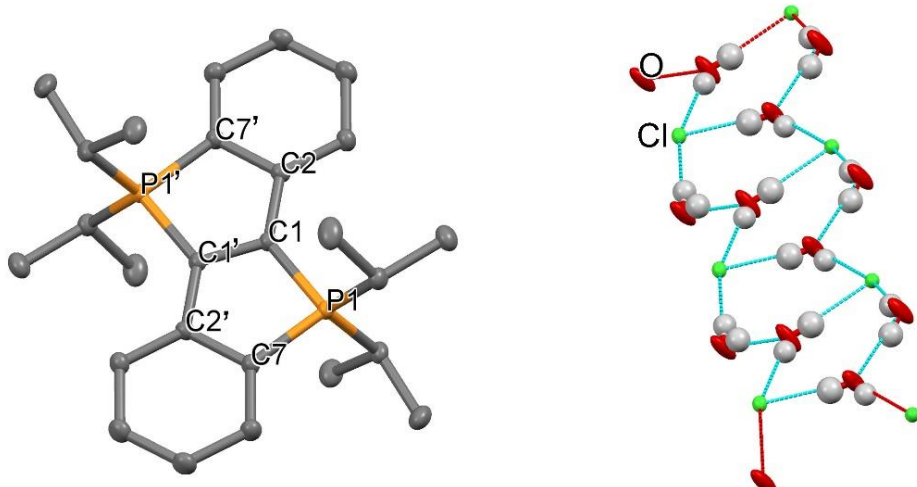


Figure S44. Left: Mercury plot of the dicationic fragment of **6b**·4 H₂O (displacement ellipsoids drawn at 50% probability, hydrogen atoms and co-crystallized water molecules omitted for clarity). Selected bond lengths (\AA) and angles ($^\circ$): P1–C1 1.8050(12), P1–C7 1.7948(12), C1–C1' 1.364(2), C1–C2 1.4650(15), C2–C7' 1.4122(16), C7–P1–C1 92.78(5), C1'–C1–P1 108.84(11), C1'–C1–C2 116.57(13), C2–C1–P1 134.59(8), C7'–C2–C1 112.03(10), C2'–C7–P1 109.78(8). Right: Part of the infinite hydrogen-bonded network of Cl⁻ ions and water molecules between the organic molecules (within the channels along the b axis).

Table S9. Crystal data and details of the structure determinations for **4b**, **5b·2 C₂H₄Cl₂**, **6a** and **6b·4 H₂O**.

Compound	4b	5b·2 C₂H₄Cl₂	6a	6b·4 H₂O
Empirical Formula	C ₂₆ H ₃₆ P ₂	C ₃₀ H ₄₄ Cl ₅ P ₂	C ₃₈ H ₂₈ F ₁₂ P ₄	C ₂₆ H ₄₄ Cl ₂ O ₄ P ₂
Formula Weight	410.49	643.84	836.48	553.45
Crystal system	monoclinic	monoclinic	triclinic	monoclinic
Space group	<i>P</i> 2 ₁ / <i>c</i>	<i>P</i> 1 2 ₁ / <i>c</i> 1	<i>P</i> -1	<i>P</i> 2 ₁ / <i>c</i>
<i>a</i> /Å	15.61085(17)	20.86081(18)	8.5220(2)	11.58860(14)
<i>b</i> /Å	13.32989(13)	7.69082(8)	9.9411(2)	7.60155(9)
<i>c</i> /Å	11.76973(13)	21.0550(2)	11.2621(3)	16.9635(2)
α /°	90	90	108.613(2)	90
β /°	106.1572(11)	97.3326(8)	92.321(2)	104.1693(12)
γ /°	90	90	102.393(2)	90
V /Å ³	2352.43(4)	3350.36(6)	876.99(4)	1448.87(3)
<i>Z</i>	4	4	1	2
<i>F</i> ₀₀₀	888	1356	424	592
<i>d</i> _c /Mg·m ⁻³	1.159	1.276	1.584	1.269
μ /mm ⁻¹	0.194	0.547	0.309	0.363
max, min transmission factors	1.000, 0.444 ^a	1.0000, 0.8924 ^b	1.000, 0.902 ^a	1.000, 0.808 ^a
X-ray radiation, λ /Å	Mo- $K\alpha$, 0.71073	Mo- $K\alpha$, 0.71073	Mo- $K\alpha$, 0.71073	Mo- $K\alpha$, 0.71073
data collect. temperature /K	120(1)	120(1)	120(1)	120(1)
θ range /°	2.4 - 32.4	2.3 - 34.7	2.2 - 34.8	2.5 - 32.4
index ranges <i>h</i> , <i>k</i> , <i>l</i>	±23, -19 ... 20, -16 ... 17	-32 ... 33, ±12, ±33	±13, ±15, -18 ... 17	±17, -10 ... 11, ±25
reflections measured	93035	225895	28230	50915
unique [<i>R</i> _{int}]	8230 [0.0323]	14171 [0.0638]	7263 [0.0413]	5059 [0.0381]
observed [<i>I</i> > 2σ(<i>I</i>)]	7770	11123	5540	4645
parameters refined [restraints]	261 [0]	342 [0]	286 [0]	174 [0]
GooF on <i>P</i> ²	1.167	1.027	1.041	1.106
<i>R</i> indices [<i>F</i> ₀ >4σ(<i>F</i> ₀)] <i>R</i> (<i>F</i>), <i>wR</i> (<i>P</i> ²)	0.0444, 0.1050	0.0581, 0.1502	0.0449, 0.0982	0.0413, 0.0966
<i>R</i> indices (all data) <i>R</i> (<i>F</i>), <i>wR</i> (<i>P</i> ²)	0.0481, 0.1068	0.0770, 0.1624	0.0659, 0.1088	0.0463, 0.0989
difference density: max, min /e·Å ⁻³	0.527, -0.237	2.595, -1.511	0.477, -0.329	0.786, -0.458
deposition number CCDC	1884989	1884990	1884991	1884992

^a numerical absorption correction. ^b semi-empirical absorption correction.

References

- (1) (a) Riss, A.; Wickenburg, S.; Gorman, P.; Tan, L. Z.; Tsai, H.-Z.; de Oteyza, D. G.; Chen, Y.-C.; Bradley, A. J.; Ugeda, M. M.; Etkin, G.; Louie, S. G.; Fischer, F. R.; Crommie, M. F., *Nano Letters* **2014**, *14*, 2251-2255. (b) Bentley, K. W.; de los Santos, Z. A.; Weiss, M. J.; Wolf, C., *Chirality* **2015**, *27*, 700-707.
- (2) (a) Kowalik, J.; Tolbert, L. M., *J. Org. Chem.* **2001**, *66*, 3229-3231. (b) Okamoto, K.; Omoto, Y.; Sano, H.; Ohe, K., *Dalton Trans.* **2012**, *41*, 10926-10929.
- (3) Gardecki, A. J.; Maroncelli, M., *Appl. Spectroscopy* **1998**, *52*, 1179-1189.
- (4) Melhuish, W. H., *J. Phys. Chem.* **1961**, *65*, 229-235.
- (5) (a) Gaussian 09, Revision B.01 and Revision D.01, Frisch, M. J.; Trucks, G. W.; Schlegel, H. B.; Scuseria, G. E.; Robb, M. A.; Cheeseman, J. R.; Scalmani, G.; Barone, V.; Petersson, G. A.; Nakatsuji, H.; Li, X.; Caricato, M.; Marenich, A. V.; Bloino, J.; Janesko, B. G.; Gomperts, R.; Mennucci, B.; Hratchian, H. P.; Ortiz, J. V.; Izmaylov, A. F.; Sonnenberg, J. L.; Williams-Young, D.; Ding, F.; Lipparini, F.; Egidi, F.; Goings, J.; Peng, B.; Petrone, A.; Henderson, T.; Ranasinghe, D.; Zakrzewski, V. G.; Gao, J.; Rega, N.; Zheng, G.; Liang, W.; Hada, M.; Ehara, M.; Toyota, K.; Fukuda, R.; Hasegawa, J.; Ishida, M.; Nakajima, T.; Honda, Y.; Kitao, O.; Nakai, H.; Vreven, T.; Throssell, K.; Montgomery, J. A., Jr.; Peralta, J. E.; Ogliaro, F.; Bearpark, M. J.; Heyd, J. J.; Brothers, E. N.; Kudin, K. N.; Staroverov, V. N.; Keith, T. A.; Kobayashi, R.; Normand, J.; Raghavachari, K.; Rendell, A. P.; Burant, J. C.; Iyengar, S. S.; Tomasi, J.; Cossi, M.; Millam, J. M.; Klene, M.; Adamo, C.; Cammi, R.; Ochterski, J. W.; Martin, R. L.; Morokuma, K.; Farkas, O.; Foresman, J. B.; Fox, D. J., *Gaussian, Inc.*, Wallingford CT, **2016**. (b) Glendening, E. D.; Badenhoop, J. K.; Weinhold, F., *J. Comp. Chem.* **1998**, *19*, 628-646. (c) Glendening, E. D.; Landis, C. R.; Weinhold, F., *WIREs Comput. Mol. Sci.* **2012**, *2*, 1-42.
- (6) (a) Becke, A. D., *J. Chem. Phys.* **1993**, *98*, 5648-5652. (b) Lee, C.; Yang, W.; Parr, R.G., *Phys. Rev. B* **1988**, *37*, 785-789. (c) Vosko, S. H.; Wilk, L.; Nusair, M., *Can. J. Phys.* **1980**, *58*, 1200-1211. (d) Stephens, P. J.; Devlin, F. J.; Chabalowski, C. F.; Frisch, M. J., *J. Phys. Chem.* **1994**, *98*, 11623-11627.
- (7) Weigend, F.; Ahlrichs, R., *Phys. Chem. Chem. Phys.* **2005**, *7*, 3297-305.
- (8) Grimme, S.; Antony, J.; Ehrlich, S.; Krieg, H., *J. Chem. Phys.* **2010**, *132*, 154104.
- (9) (a) Neese, F., *WIREs Comput. Mol. Sci.* **2012**, *2*, 73-78, 10.1002/wcms.81. (b) Neese, F., *WIREs Comput. Mol. Sci.* **2018**, *8*, e1327, 10.1002/wcms.1327.
- (10) (a) Tomasi, J.; Mennucci, B.; Cammi, R., *Chem. Rev.* **2005**, *105*, 2999-3094. (b) Scalmani, G.; Frisch, M. J., *J. Chem. Phys.* **2010**, *132*, 114110.
- (11) (a) Rahalkar, A.; Stanger, A., Aroma, <http://chemistry.technion.ac.il/members/amnon-stanger>. (b) Stanger, A., *J. Org. Chem.* **2006**, *71*, 883-893. (c) Stanger, A., *J. Org. Chem.* **2010**, *75*, 2281-2288. (d) Gershoni-Poranne, R.; Stanger, A., *Chem. Eur. J.* **2014**, *20*, 5673-5688.
- (12) Yanai, T.; Tew, D.; Handy, N., *Chem. Phys. Lett.* **2004**, *393*, 51-57.
- (13) Kabsch, K., in: Rossmann, M. G.; Arnold, E. (Eds.) "International Tables for Crystallography" Vol. F, Ch. 11.3, Kluwer Academic Publishers, Dordrecht, The Netherlands, **2001**.
- (14) (a) CrysAlisPro, Agilent Technologies UK Ltd., Oxford, UK **2011-2014**. (b) Rigaku Oxford Diffraction, Rigaku Polska Sp.z o.o., Wrocław, Poland **2015-2018**.
- (15) (a) SCALE3 ABSPACK, CrysAlisPro, Agilent Technologies UK Ltd., Oxford, UK **2011-2014**. (b) Rigaku Oxford Diffraction, Rigaku Polska Sp.z o.o., Wrocław, Poland **2015-2018**.
- (16) Blessing, R. H., *Acta Cryst.* **1995**, *A51*, 33-38.
- (17) Busing, W. R.; Levy, H. A., *Acta Cryst.* **1957**, *10*, 180-182.
- (18) (a) Palatinus, L., SUPERFLIP, EPF Lausanne, Switzerland. (b) Fyzikální ústav AV ČR, v. v. i., Prague, Czech Republic, **2007-2014**. (c) Palatinus, L.; Chapuis, G., *J. Appl. Cryst.* **2007**, *40*, 786-790.
- (19) (a) Sheldrick, G. M., SHEXL-20xx, University of Göttingen and Bruker AXS GmbH, Karlsruhe, Germany **2012-2018**. (b) Sheldrick, G. M., *Acta Cryst.* **2008**, *A64*, 112-122. (c) Sheldrick, G. M., *Acta Cryst.* **2015**, *C71*, 3-8.